ALMA MATER STUDIORUM
UNIVERSITY OF BOLOGNA
SCHOOL OF SCIENCE

Laurea Magistrale in Analisi e Gestione dell'Ambiente
Curriculum in Water and Coastal Management

Characterization of vegetation patterns in a Venice lagoon saltmarsh from drone-based hyperspectral remote sensing

Thesis in: Advanced technologies and decision support systems in water and coastal management

Supervisor
Sonia Silvestri

Presented by:
Olinda Rufo

Co-supervisor
Tegan Blount

Unique session Academic year 2021-2022

ACKNOWLEDGEMENT

My heart is thankful to God who gave me the strength to write this thesis. Thank you to my supervisor **Prof. Sonia Silvestri**, from the Department of Biological, Geological and Environmental Sciences, University of Bologna, for your patience, guidance, and support. I have benefited greatly from your wealth of knowledge and meticulous editing. I am extremely grateful that you took me on as a student on to work on this project.

Thank you to my co-supervisor **Ms. Tegan Blount** and **Mr. Marco Assiri**, for their continuous support during my thesis and great help with research and data analysis.

My deepest gratitude to the **WACOMA administrative team** for the help and support during these 2 academic years.

TABLE OF CONTENTS

LIST OF FIGURES

LIST OF TABLES

ACRONYMS

AGB	Above Ground Biomass
BGB	Below Ground Biomass
C	Carbon
CC	Climate Change
DIC	Dissolved Inorganic Carbon
DOC	Dissolved Organic Carbon
DOM	Dissolved Organic Matter
EM	Electromagnmetic
EMR	Electromagnetic Radiation
GEMI	Global Environmental Index
GPP	Gross Primary Productivity
GPS	Global Position System
LOI	Loss on Ignition
MSAVI	Modified Soil-Adjusted Index
NDVI	Normalized Difference Vegetation Index
NIR	Near Infrared
NPP	Net Primary Productivity
OC	Organic Carbon
POC	Particular Organic Carbon
Rc	Carbon respired back to the atmosphere
Rwater	Respired from the water system
RS	Remote Sensing
SLR	Sea Level Rise
SAVI	Soil-adjusted Vegetation Index
VI	Vegetation Index

ABSTRACT

Coastal wetlands are unique and complex geomorphological systems that respond to a wide range of changing influences, and their responses remain poorly understood, emphasizing the need for and importance of this study. These ecosystems provide useful feedbacks to coastal systems, such as soil stabilization and coastal protection. They are very important carbon sinks. For carbon to be stored in the soils there must be biomass that is produced. This study focuses on the above ground biomass and the below ground biomass in the saltmarsh in order to evaluate the amount of organic matter that is stored in the soils. To obtain this, field campaigns were conducted to sample the above ground vegetation and core samples to analyse the amount of vegetation biomass and carbon stock in the soil. The marsh selected for this study is characterized by three different levels of elevation, high mid and low. We found that the middle marsh is the area that stores the highest amount of organic matter in the soil as compared to the lower and the higher marsh. In addition, we found that there is a linear positive correlation between the AGB and the BGB. Furthermore, the study concludes that it is possible to use vegetation indices retrieved from remote sensing to characterize the biomass. The NDVI (Normalized Difference Vegetation index) demonstrated to be a good proxy for the AGB only for low and mid-marsh vegetation species, while it saturates for high-marsh high-biomass vegetation. Studying the distribution of the NDVI ranges across the studied marsh, we found that it is mainly covered by dense vegetation, with AGB biomass larger than 400 g/m2.

.

Keywords: above-ground biomass, below-ground biomass, bulk density, organic carbon, hyperspectral imaging, vegetation index, NDVI

Chapter 1

1. INTRODUCTION

1.1. Definition and Importance of coastal wetlands

For many decades, the definition of wetlands has been adjusted to account for all the different types of wetlands. In general, wetlands are areas where water covers the soil, or is present either at or near the surface of the soil all year or for varying periods of time during the year, including during the growing season. Water saturation largely determines how the soil develops and the types of plant and animal communities living in and on the soil. Wetlands may support both aquatic and terrestrial species. The prolonged presence of water creates conditions that favor the growth of specially adapted plants and promote the development of characteristic wetlands soils (US EPA, 2015).

Tidal salt marshes are wetland ecosystems that form in areas covered by saltwater at high tide and exposed to the air at low tide, and this tidal cycle happens once or twice each day depending on the tidal regime (Schwirzer, 2008). Wetlands perform many processes simultaneously and therefore they provide a group of values to humans. In addition, its own value is defined at three levels of ecological hierarchy; namely population, ecosystem, and biosphere Table 1-1 -(Mitsch and Gosselink, 2000).

Table 1-1 General categories of wetland values at three different ecological scales (from (Mitsch and Gosselink, 2000)

Ecological scale	Value
Population	Animals harvested for pelts
	Waterfowl and other birds
	Fish and shellfish
	Timber and other vegetation harvest
	Endangered/threatened species
Ecosystem	Flood mitigation
	Storm abatement
	Aquifer recharge
	Water quality improvement
	Aesthetics
	Subsistence use
Biosphere	Nitrogen cycle
	Sulfur cycle
	Carbon cycle
	Phosphorus cycle

Consequently, they are considered one of the most dynamic ecosystems with plant communities that are situated on sheltered coastlines ranging geographically from the sub-arctic to the tropics and occurring most extensively in temperate zones Sifleet et al., 2011). These environments accommodate different halophyte plant species that group into communities of vegetation types according to their potential to salt-tolerance and soil moisture (Fig. 1-1).

Another well-known characteristic of such types of environments is that they have poor drainage capacity which results in saturated soils, and they provide habitat for wetland-dependent plants and animals whose life cycle depends on salty environments (Chapman, 1976; Marani et al., 2003; Silvestri et al., 2005). In addition, the general morphological benefits of saltmarshes expand to flood reduction, and coastal protection which is achieved through a constant exchange of mineral sediments from the interaction of tides and fluvial contributions (Owers et al., 2020) resulting in sediment accretion, and nutrient cycling. In this manner, the identification of sources of organic carbon in saltmarsh ecosystems is important for evaluating their effectiveness in the carbon cycle (Krause et al., 2022)

Furthermore, the ability of these ecosystems in providing protection is entirely dependent on the growth and dimension of the salt marsh. One such indicator of this tidal frame growth is the distribution of vegetation that is promoted by tidal inundation which consequently influences various factors such as soil salinity, anoxia, and nutrient availability (Adame and Lovelock, 2011; Chen and Twilley, 1999; Feller et al., 2010; Rogers et al., 2017). In addition, the degree of wetness influences the type of vegetation that is established in the salt marsh. In the most inundated zones, organic matter accumulates due to hipoxyc conditions that prevent plant material decomposition (Bouma et al., 2005; Kirwan et al., 2016; Kirwan and Megonigal, 2013; Mudd et al., 2009; Turner et al., 2004). Moreover, several studies (Alongi, 2014; Barbier et al., 2011; Chmura et al., 2003; Lovelock and Duarte, 2019) have identified that coastal wetlands (including saltmarshes) as a global value for organic carbon sequestration, due to their ability to inhibit aerobic microbial breakdown which limits the release of greenhouse gases to the atmosphere (Fourqurean et al., 2012; Kristensen et al., 2008). The carbon stocked in coastal systems and salt marshes is called “blue carbon” (Mcleod et al., 2011).

In fact, wetland ecosystems such as salt marshes and mangrove forests have an important role in climate regulation through capturing and preserving great amounts of carbon that regulates anthropogenic CO2 emissions. This is achieved because of their carbon-rich ecosystems. Although, mangroves forests store more carbon (compared to salt marshes), salt marshes sequester proportionally more (24%) net primary production (NPP) than mangroves (12%) (Alongi, 2014). However, global projections have illustrated major coastal wetland reductions of 20-90% under the consequence of sea-level rise SLR, (Blankespoor et al., 2014; Spencer et al., 2016) and salt marshes are not excepted from the long-term changes that arise from sea-level, mainly because of their vulnerability due to where saltmarsh are located.

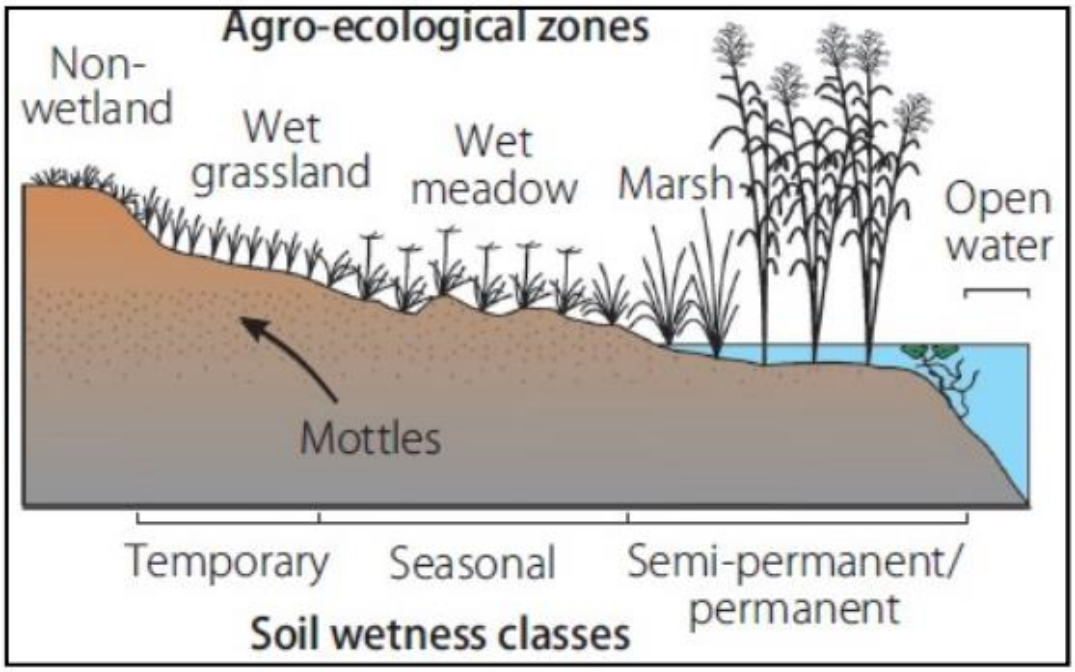

Figure 1-1 Vegetation zonation in a wetland along a profile (Source: Kotze et al. 1994)

1.2. Adaptive capacity of Saltmarsh vegetation to sea-level rise

Salt marshes can resist the short-term stress during storm events when sediment is suspended from tidal flats (Borsje et al., 2011). In some cases, this provides enough sediment to be trapped by the vegetation, which allows salt marshes to grow with the rising of the water level and adapt to changing of SLR conditions (e.g., Best et al., 2018; Kirwan et al., 2016, 2010). The sedimentation of these sediments creates more room for vegetation to grow and acts as a defense mechanism to reduce wave-induced erosion (Feagin et al., 2009; Wang et al., 2017). The vegetation generate a rhizome network and roots, which can prevent erosion and contribute to the depositional of suspended organic matter (OM) in the soil (Gacia and Duarte, 2001). The OM that is deposited can either be produced within the habitat (autochthonous) or originate from a different source (allochthonous), which in turn can be consumed by heterotrophic organisms and or mineralized releasing CO2 depending on the conditions (Kennedy et al., 2010). The process of mineralization occurs when the oxygen present in the soils is consumed in the upper 30 cm of the sediment.

Some studies (Schuerch et al., 2013; Temmerman et al., 2004) have analyzed the vertical growth of salt marshes, as influenced by sediment supply, and in-depth knowledge on plant zonation obtained from field and modelling studies in temperate zones is well developed (Silvestri et al., 2005). A marsh is mainly characterized by halophytic vegetation (salt-tolerant), however, they do not all depend on the saline environment for their growth, in fact some species grow in conditions that are not saline (glycophytes vegetation) (Silvestri and Marani, 2004). The most contributing factor to the growth of a saltmarsh is the balance and exchange between sediment transport processes, soil subsidence, sea level rise and vegetation dynamics (Ursino et al., 2004). When there is enough inorganic

sediment deposition occurring due to tidal inundations, this grants the marsh's topographic elevation to increase and creates more room for plants to grow while the roots of the plants firm the deposited on the soil (Pethick, 1995). When this happens, other vegetation species also colonize the soil, and because of the saline conditions in the environment these vegetations grow according to their salt tolerance capacity and tolerance to floods, creating organized characteristic patches of vegetation on the marsh (Silvestri and Marani, 2004). An example of the zonation process can be seen in Figure 1-2.

Figure 1-2 Zonation boundaries observed in the lagoon of Venice: *Spartina anglica* (light green vegetation surrounding the water) is surrounded by *Limonium narbonense* (outer part). The plants compete for limited biotic resources, for favorable growing conditions.

The driving abiotic factors leading to zonation include: water dynamics, nutrient uptake (Ungar, 1991), light intensity availability, aerobic condition within the soil (tidal salt-marsh flooding affects oxygen availability and changes soil chemistry) and grazing, caused by herbivore insects (Ellison, 1987). Various studies (Hodáňová, 1981; Snow and Vince, 1984; Ungar, 1991) reveal that the best competitors dominate the least stressful habitats, leaving the poor competitors to more stressful zones.

1.3. Mechanisms of Carbon Storage in Saltmarsh

Salt marshes are environments rich in carbon (C) in their sediments. Capturing and trapping large amounts of CO2, they play an important role in climate regulation and

biogeochemical cycling (Alongi, 2020a). Due to drastic climatic changes, the ability to estimate and monitor carbon stocks has become important to adapt and mitigate the consequences. Existing literature shows that abundant vegetation units of mangrove and saltmarsh store large quantities of organic carbon in their soils (e.g. Adame et al., 2013; Kelleway et al., 2016; Lovelock et al., 2013; Saintilan et al., 2013). However previous sampling protocols (IPCC, 2014) have not adequately recognised the importance of vegetation when addressing C storage, although both ecosystems have similarities and differences in C cycling in global coastal oceans. It is therfore important to unveil the various sources and principal processes that contribute towards storage of organic C in wetlands, particularly in saltmarsh soils. This is one of the main purposes of this study. Soils are an integral part of the C cycle: C enters the soil through sequestration as plants and animals' decay enriching the soil of organic matter. Part of the C contained in the organic matter is prevented from being oxidized to CO2 (greenhouse gas) under hypoxic conditions and therefore it is not released to the atmosphere. In this way, the more the hypoxic sediment conditions are available beneath salt marshes, the more total amount of C is stored in them (Sifleet et al.,). Saltmarsh soils rich in C are capable of reaching an estimated depth from less than a half a meter to over 7 m (Brevik and Homburg, 2004a).

Salt marshes and mangrove forests store large quantities of organic carbon (CORG) in soils and, although in smaller proportion, in plant biomass. According to (Alongi, 2020a), salt marshes store carbon at a faster rate than mangrove because of the difference in the ecosystem age, intertidal position, species composition and in terms of geographic, and environmental factors. Other studies of marshes in the US, Belgium and the Netherlands, (Craft, 2007) and (Van de Broek et al., 2016) respectively, discovered that marshes located more upstream along estuaries predominantly receive riverine inputs, characterized by high SPM and OC contents (thus leading to higher sedimentation rates) and have higher rates of SOC accumulation and higher SOC stocks.

An estimate of the median CORG stocked in salt marshes and mangrove forests in the above and belowground plant biomass and in soils within the first 1 m is shown in the Figure 1.3.

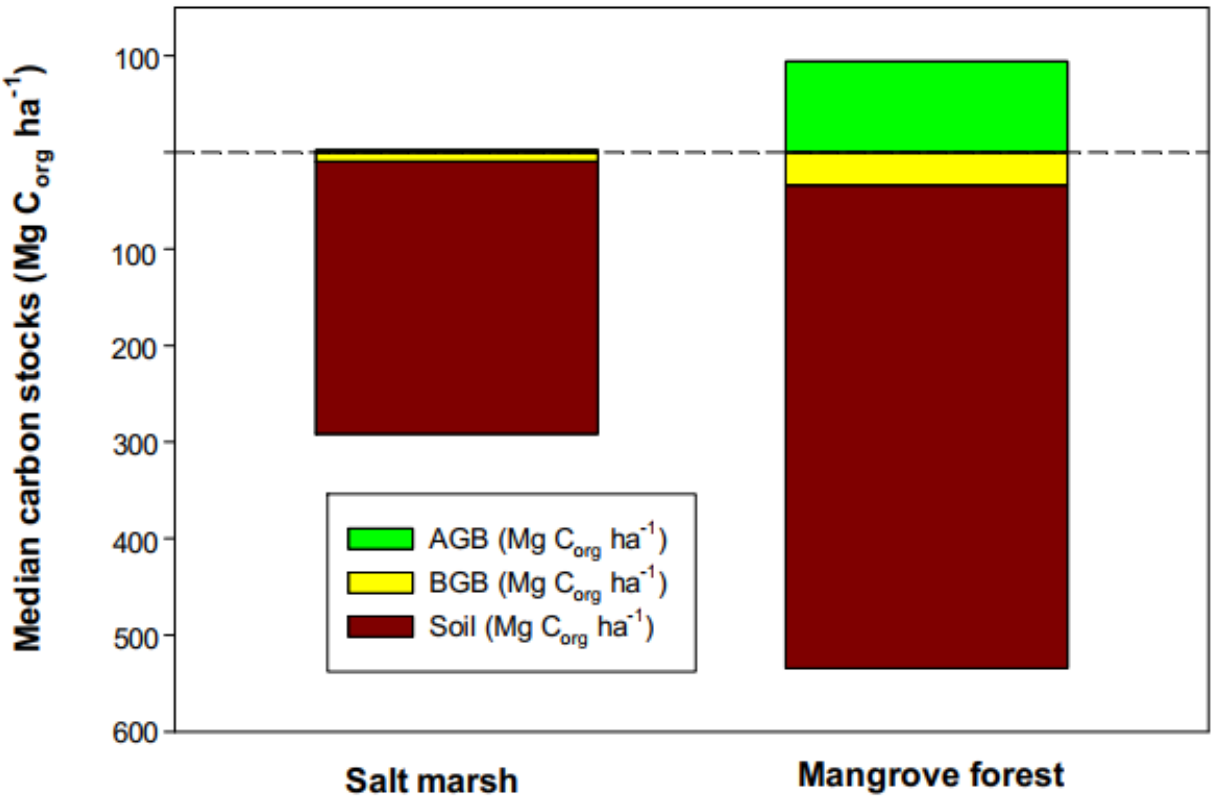

Figure 1-3 Distribution of organic carbon stocks in above- and below-ground plant biomass and in soils to a depth of 1 m in salt marshes and mangroves *(Alongi, 2020)*

Figure 1.3 shows that mangroves forest store more C in the belowground biomass (BGB) as well as in the soil, and account for twice of total C stored in saltmarshes. Moreover, globally, mangroves cover larger geographic areas of the world. In contrast, salt marshes exhibit greater rates of belowground root production, while mangroves have greater rates of aboveground biomass production.

The pathways of C flow in saltmarshes are summarized and presented in Figure 1.4. The figure illustrates CORG pool (both alive and dead roots and other organic matter) in soils in a marsh floor with units of Tg of CORG. The process begins when there is an increased topographic elevation due to soil deposition from tidal flats, which allows vegetation to be establish on the marsh (Silvestri and Marani, 2004). The production of new roots, branches and leaves reflects primary production (GPP) which is partly respired back into the atmosphere (RC) in the form of CO2. All the remaining organic carbon stored in the saltmarsh represent net primary production (NPP) (Alongi, 2020). The above and belowground biomass containing organic C is accumulated in the marsh soil layer, which in turn becomes the autochthonous sediment organic carbon (SOC). However, not all the autochthonous OC is stored in the sediments: some is exported to the adjacent coastal or estuarine water body via tides, winds and porewater exchange in the form of dissolved organic carbon (DOC) and particulate organic carbon (POC) which are eventually respired from the water system (Rwater) or buried in adjacent ecosystems such as seagrass beds (Alongi, 2014). When there is supersaturation of adjacent tidal waters, especially in freshwater and brackish-water anaerobic systems, a chain of reactions contributes to a series of chemical changes and CH4 may be released to the atmosphere. All these

processes involving the tidal inundation, OM decomposition, position of the saltmarsh along land-to-sea gradient permits the continual burial of organic matter making the environment biogeochemically active (Kusumaningtyas et al., 2019)

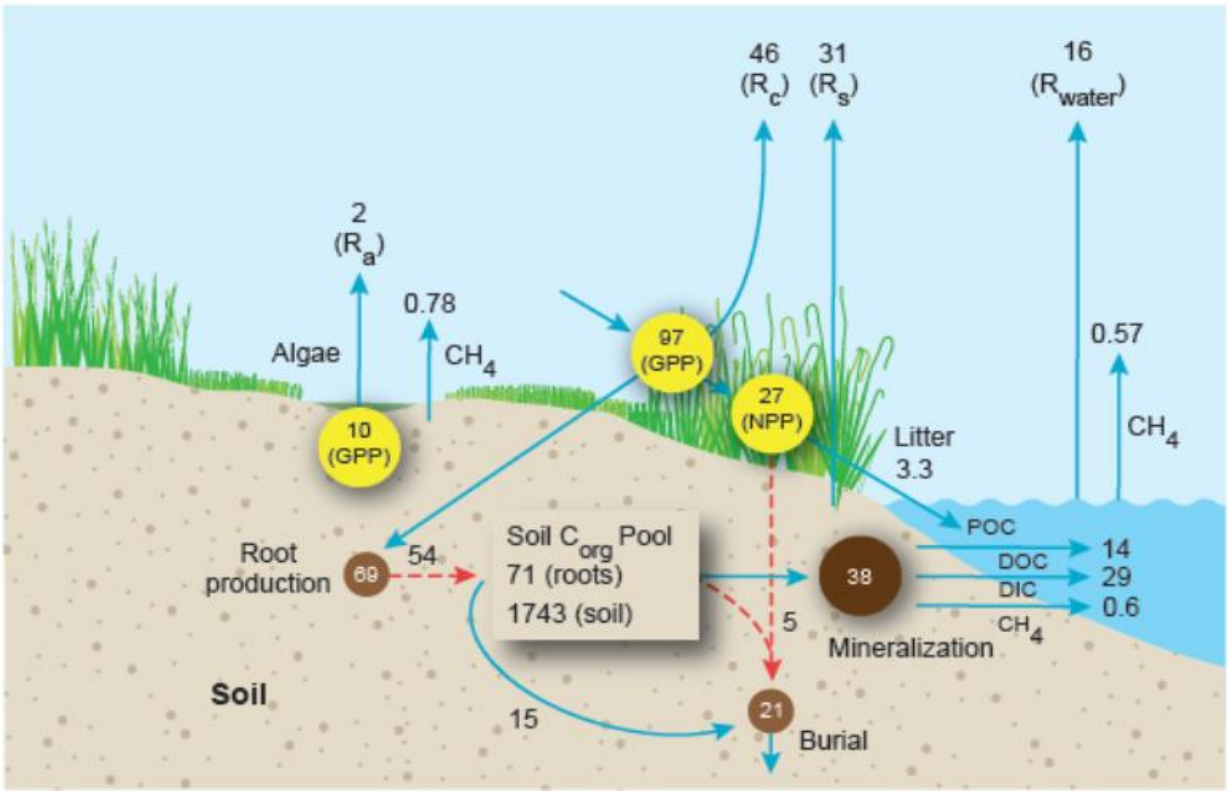

Figure 1-4 Major pathway of carbon flow through saltmarsh ecosystem. All values are in Tg C y−1 (source: Alongi, 2014). Please refer to the above text for abbreviations.

1.4. Geographic Information System

Geographic Information Systems (GIS) can be referred to as a set of databases of numerical data that are associated with spatial properties that help to identify patterns or the exact location of objects. GIS is very important when it comes to observing the Earth. It gives access to reliable, detailed, timely, and affordable geospatial data that can be used for various purposes such as generating maps and taking decisions based on them (Tempfli et al., 2009). In order to achieve these geospatial data, there are four different resolution types of data that allow to quantitatively measure factors such as color, space, and detail. The types of data are spatial, spectral, radiometric, and temporal.

1.5. Remote Sensing

Remote sensing is a tool that allows the collection of many global data using sensors that do not have direct contact with the Earth's surface and in a cost-effective way. (Tempfli et al., 2009) defines remote sensing as the art, science, and technology of observing an object, scene, or phenomenon by instrument-based techniques. The technique provides extremely valuable observations on large areas that are difficult to do *in-situ* surveys. Remote sensing makes use of the electromagnetic energy captured by sensors to detect various surfaces on Earth. Electromagnetic energy is composed of waves that oscillate in the electric and magnetic fields. These types of waves have amplitudes, wavelengths, and frequencies, and different frequencies of electromagnetic waves produce different kinds of

light and they all move at the speed of light (Tempfli et al., 2009). The visible portion of the electromagnetic spectrum goes from about 350 nm to 700 nm, hence including the wavelengths corresponding to different colors (from blue to red). Wavelengths greater than 700 nm are in the near-infrared (NIR) portion of the spectrum, followed by infrared, microwaves, and radio waves; on the other side, wavelengths shorter than 350 nm include UV radiation, X-rays, or Gamma rays (Tempfli et al., 2009). All these are collectively referred to as electromagnetic radiation as shown in Figure 1-5.

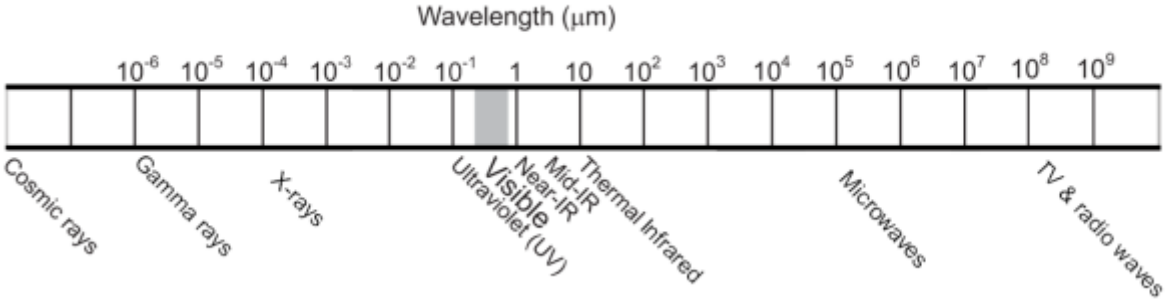

Figure 1-5 Electromagnetic spectrum (Tempfli et al., 2009)

Only the visible wavelengths produce colors that we can dictate with our eyes. This portion is a very small part of the EM spectrum. However, there are sensors that have been designed to detect other wavelengths that we cannot see (Klemas et al., 2003), including NIR for example.

1.6 Passive and active sensors

Figure 1-6 illustrate also the two different types of sensors: passive and active. Passive sensors that observe the Earth measure solar or terrestrial energy emitted or reflected by the Sun. In areas where the energy coming from the Sun is not available, a different source of energy is needed, that is why we use active sensors. Active sensors are also useful where cloud cover interferes with the transmission of the signal, and they are useful also at night. Active sensors detect returning energy from the target object or surface. Examples of the imagery produced are RADAR and LiDAR.

1.7 Spectral resolution

Remote sensing sensors are built to detect different portions of the EM spectrum, and this is based on the types of applications that one wants to obtain. Each portion of the EM spectrum detected by the sensor is referred to as “band” or “channel”. When the sensor detects the EM radiation, it converts the signal to a “digital number”, which is a quantity proportional to the intensity of the electromagnetic signal. This value is then transformed into “radiance” (W/m^2 sr μm) and consequently to “reflectance”, which is the ratio between the radiance reflected by the target and the irradiance coming from the Sun. This process is repeated for each band that the sensor detects.

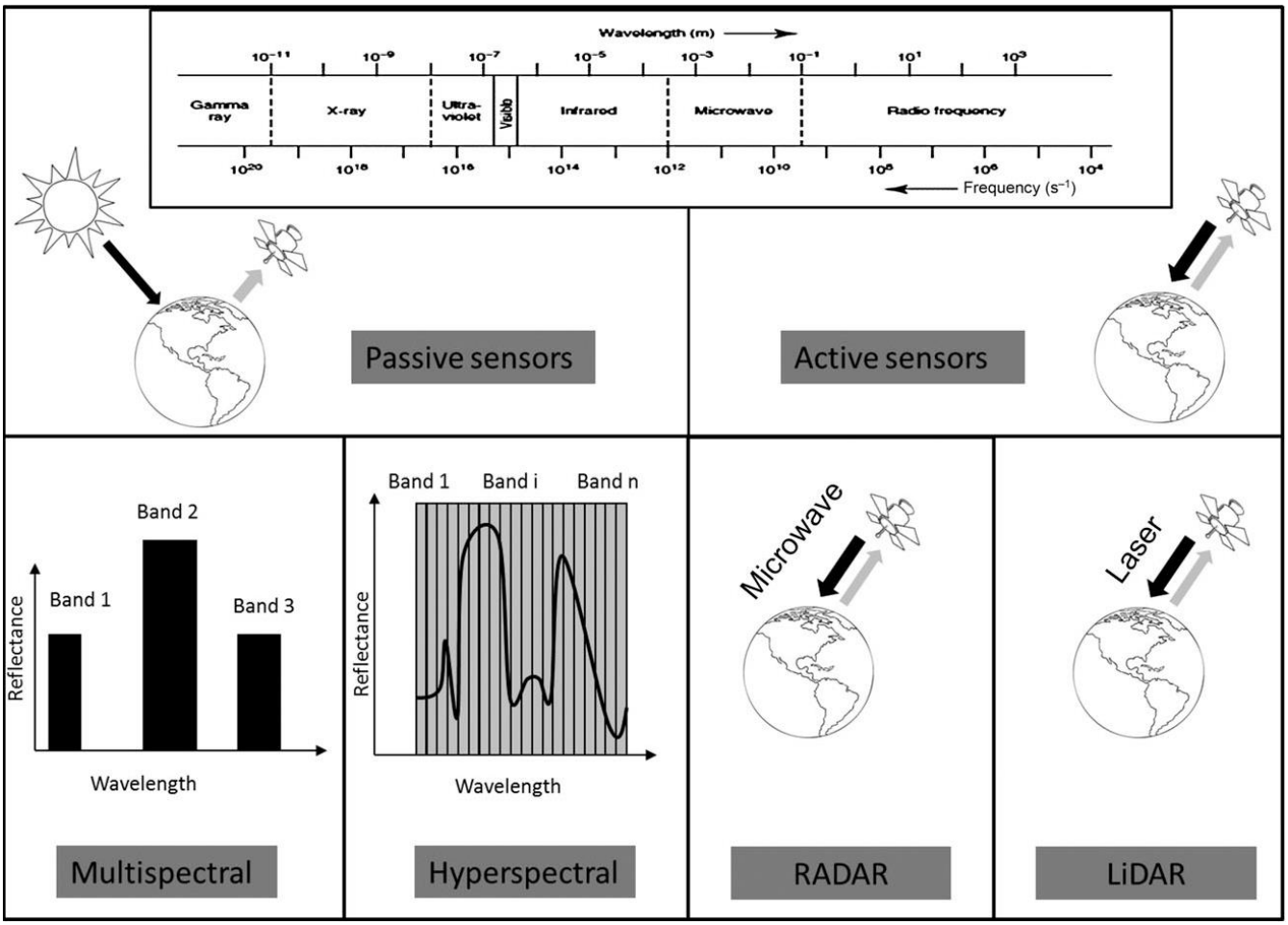

Figure 1-6 Difference between active and passive sensors (Pettorelli et al., 2014)

The accuracy in which the Earth can be observed with satellite depends primarily on the different characteristics of their sensors. These sensors properties control how detailed the information about the surface can be. As already mentioned, the sensors used in remote sensing detect wavelength ranges in specific spectral bands or channels. This property is called “spectral resolution” (Tempfli et al., 2009). The spectral resolution of a sensor increases with the number of channels in which it can receive ranges of the EM spectrum (Roy, 1989). Such increase provides information about the ability to reproduce the spectral properties of a surfaces as accurate as possible by allowing the number of bands obtained by remote sensing to increase and the bandwidth to be narrower with the increasing resolution. Different materials on the earth have a unique spectral signature, meaning that they absorb and reflected light from different wavelengths differently (Xue and Su, 2017). In this way, objects can be distinguished from one another by looking at the reflection behavior. If a sensor has more spectral channels, it allows the spectral signatures of objects to be seen with better precision (Bell and Callow, 2020). For instance, by looking at spectral signatures of vegetation, it is possible to differentiates between healthy and stressed vegetation as they have different absorption behavior.

Multispectral sensors capture reflected energy within several specific broad bands (ranginging between 3 and 20), while hyperspectral sensors capture hundreds of bands resulting in a relatively continuous measurement of a portion of the electromagnetic spectrum (Pettorelli et al., 2014). Many satellites observing the Earth are equipped with

multispectral sensors. Examples of modern multispectral sensors are the MSI on board of Sentinel 2, that collect information in 12 bands, and the OLI sensor on board of Landsat-9. Each band does not just correspond to one wavelength, instead it picks up a specific wave range and averages this information. This is important because the signal obtained from multiple wavelengths is much stronger of a single wavelength. In addition, in multipsctral sensors not all channels are adjacent to each other and this is because sometimes there are large gaps of wavelength range in the EM spectrum in which no information is collected from the sensor.

Hyperspectral imaging sensors gather data from the EM spectrum as well. As mentioned befrore, the EM spectum consists of multiple bands of EM radiations which Is separated by size and frequency. Hperspectral sensor is capable of retrieving data from 380 nm to 2500 nm. This means that it can gather data in the visible, Visible-NIR, NIT ans SWIR.

1.8 Monitoring Vegetation using Remote Sensing

To complete the overview of the use of spatial methods techniques, it is also essential to explore and discuss how the ratio of reflectance within different bands can be used to study the vegetation status. Numerous spectral vegetation indices have been developed to characterize vegetation canopies. Radiance or reflectance measurements can therefore be used to detect the presence of growing vegetation, if the position and width of the spectral bands of measuring instruments are selected in the process (Swoish et al., 2022).

The use of vegetation indices in image processing and analysis should be selected based on an understanding of their inherent strengths and limitations and their suitability for a particular application (Bell and Callow, 2020). The manual separation or identification of different vegetation canopies is challenging, especially in regions of high-density vegetation growth (Bell and Callow, 2020). Nevertheless, these limitations suggested that higher spectral resolution creates the opportunity to study sites in a detailed and distinguished manner (Klemas, 2011). Furthermore, with the technological evolution, other recent alternatives with high spectral resolution combined with high spatial resolution such as drone imagery can support segmentation of individual species in areas where vegetation distribution are not spatially discrete (Bell and Callow, 2020).

Vegetation Indices

Remote sensing of vegetation is mainly performed by obtaining the electromagnetic reflectance information from canopies using passive sensors (Xue and Su, 2017). This reflectance can then be used to calculate vegetation indices.

According to (Roy, 1989) the reflectance of a vegetation is influenced by the reflectance characteristics of individual plant organs, canopy organization, type and growth stage of plants and structure and texture of the canopies. All these aspects provide a true reflectance characteristic. Later, Oliveira et al. (2009) affirmed that the qualitative and quantitative detention of green vegetation is one of the most important contributions of remote sensing to environmental studies. Therefore, various vegetation indexes have been developed. The most used is the NDVI (Normalized Difference Vegetation Index) which is an index which allows analyses to be carried out, at different scales, on the vegetation cover of a given region. It is an index developed to enhance the vegetation

signal with better sensitivity in regions with high biomass and better monitoring performance by decoupling the background signal from the canopy and reduce atmospheric influences (Bell and Callow, 2020).

NDVI (Normalized Difference Vegetation Index)

NDVI is the most used index for various purposes, which allows to carry out analyses, at different scales, on the vegetation cover (Rouse Jr. et al.). The index makes use of the red and near-infrared bands canopy reflectance (Huete, 1988). When calculated, the index presents a range of values between -1 and 1.

The NDVI index is calculated with the following formular:

$$1.\quad \text{NDVI} = \frac{\text{NIR}-\text{R}}{\text{NIR}+\text{R}}$$

The aim of this vegetation index is to detect the photosynthetic activity of vegetation, therefore it correlates to biomass and its canopy chlorophyll content. This index performs very well due to its sensitive response to green vegetation. However, it is inefficient when applied in areas with bare soils or soils with low vegetation cover because the soil brightness color may influence the signal as soil background. In addition, it also loses sensitivity when a canopy's area is very dense, and it requires remote sensing calibration since it is influenced by atmosphere, clouds and cloud shadow (Testa et al., 2018). In this manner, other indices have been developed to surpass these environmental factors, without succeeding.

SAVI (soil-adjusted vegetation index)

The SAVI index was found to be an important ratio combination that can describe dynamic of both soil and vegetation systems from remotely sensed data. The SAVI is an alternative to NDVI because it is refined or "calibrated" so that soil substrate variations are effectively normalized and are not influencing the vegetation measure. (Huete, 1988) Therefore, this Index was established to overcome the issues that NDVI has with soil backgrounds. A vegetated area transmits a significant amount of NIR flux towards the soil surface, irradiating the soil underneath as well as in between individual plants which is consequently sent back toward the sensor in a manner dependent upon the optical properties of thet soil surface. In this manner, it was vital to develop the soil adjusted index. The SAVI index is calculated with the following formular:

SAVI = [(NIR - red)/(NIR + red + L)] ×(I+L).

where L is the soil conditioning index, which improves the sensitivity of NDVI to soil background. The range of L is from 0 to 1. The value of L is around 0.5 under most common environmental conditions. When L is close to 0, the value of SAVI is equal to NDVI. However, L factor should vary inversely with the amount of vegetation present to obtain the optimal adjustment for the soil effect (Xue and Su, 2017)

MSAVI (Modified Soil-Adjusted Index)

This index was developed to modify the original SAVI index. MSAVI replaces L factor in the SAVI equation with a variable L function. In this way, reduces the influence of bare soil on SAVI, which can be expressed as follows:

MSAVI = 0.5 $*$ {2R800 + 1 − SQRT [(2R800 + 1)2 − 8 (R800 − R670)]}.

GEMI Global Environment Monitoring Index

GEMI index corrects for the atmospheric conditions. It is more useful to compare observations under varying atmospheric and illumination conditions, and more sensitive of actual surface conditions than NDVI over the bulk of the range of vegetation conditions. This index is calculated with the following formular:

η = [2(NIR 2 − R 2) + 1.5NIR + 0.5R] (NIR + R + 0.5)

In this thesis I will calculate the abovementioned four indices and compare the results.

SCOPE OF THE RESEARCH

Objectives of the Thesis

For many years, remote sensing applications have been a practical and cost-effective technique used to analyze the spatial and temporal evolution of the Earth surface. As for the study site selected for this thesis, various studies on the San Felice saltmarsh (Venice lagoon, Italy) have already effectively monitored the area, demonstrating the advantages of using remote sensing to develop maps and models. However, the area is characterized by high spatial complexity and temporal variability, therefore models and satellite observations must be supplemented by aircraft and field data to obtain precise and accurate information. To contribute to mapping efforts of the saltmarsh vegetation species in San Felice, the use of hyperspectral imagery from Unmanned Aerial Vehicles (UAVs) coupled with field data is used in this study to accurately contribute to efforts already made in detecting changes in the saltmarsh.

This study aims at analyzing the biomass of the different vegetation associations in the field. Data such as the bulk density and the organic matter in the soil are retrieved and used to find significant correlations with the vegetation spectra. In addition, thanks to the extremely high spectral resolution, we also aim at calculating different types of vegetation indexes to correlate with the AGB and BGB of different vegetation associations located across the sampling area. All these efforts are directed toward meeting the goals of an ongoing NSF project (NSF, 2021) focused on creating spatial models of various dynamic factors of the wetland in response to environmental changes. One of the project's aims is to include carbon budget retrieved from vegetation characteristic and biomass production, which is linked to what this specific study tries to contribute with. The project focuses on two different wetlands: 1) North Inlet, Sotuth Carolina, USA, and 2) Venice Lagoon, Italy (NSF, 2021). The project aims to capture remote aircraft data in the South Carolina marsh,

while in the Venice lagoon, hyperspectral data are retrieved and then down-scaled the data spectral resolution in order to obtain the same MS bands of the camera used in South Carolina. This will be correlated to the biomass production in the area.

Study Aim

Based on the knowledge of the author of this thesis, specific relations between aboveground and belowground parameters in saltmarshes are not fully quantified and explained in the literature. For example, there are still gaps in the quantification of the ratio of AGB vs BGB of different plant associations. The aim of this study is to combine field-based monitoring and aerial hyperspectral imagery to investigate biomass conditions and vegetation spectral indices using a stratified sampling approach; furthermore, the correlation of AGB and BGB with the organic matter stored in the saltmarsh soils is explored. Within these overall aims, potential drivers within the marsh will be considered, including vegetation type and soil stratification depths. All these research questions, together with the knowledge gaps presented, justify the rationale of this thesis.

Chapter 2

2. EXPERIMENTAL METHODOLOGIES

2.1 Study Site

Figure 2-1 The San Felice saltmarsh in the northern basin of the Venice lagoon (Italy)

The Venice Lagoon is the largest lagoon in the Mediterranean Sea, with an area of about 550 km^2. It has three inlets that connect the lagoon with the Adriatic Sea (Losso and Ghirardini, 2010). The tidal regime is semidiurnal with an average water depth of about 1.5 m and a maximum range (at the inlets) of about 70 cm around mean sea level. The studied salt marsh (Figure 2-1) is in the northern part of the lagoon, along the San Felice channel. The studied area is demarked in red and presented in Figure 2-1 and green dots are the GPS points collected across the marsh for our study. The marshes in this area cover a total area of approximately 40 km^2 and host at least twenty species of halophytes, among which the most common are *Limonium narbonense, Sarcocornia fruticosa, Spartina maritima, Salicornia veneta, Juncus maritimus,* (NSF, 2021). The channels act as drainage and recharge zones, forming patterns of preferentially aerated soils, the levees, which have favorable conditions for the plants to grow. The morphology of the marsh is composed of different soil elevations that ranges between 0 and 50 cm above mean sea level (a.m.s.l.) (Silvestri et al., 2005). The number of halophytic species present in these marshes is limited as they grow on preferential soils. The duration of inundation of salt

marsh soils is determined mainly by the elevation of the area. The frequency of flooding of the soil also affects the ecogeomorphology of the soil.

2.2 Collection of samples in the field

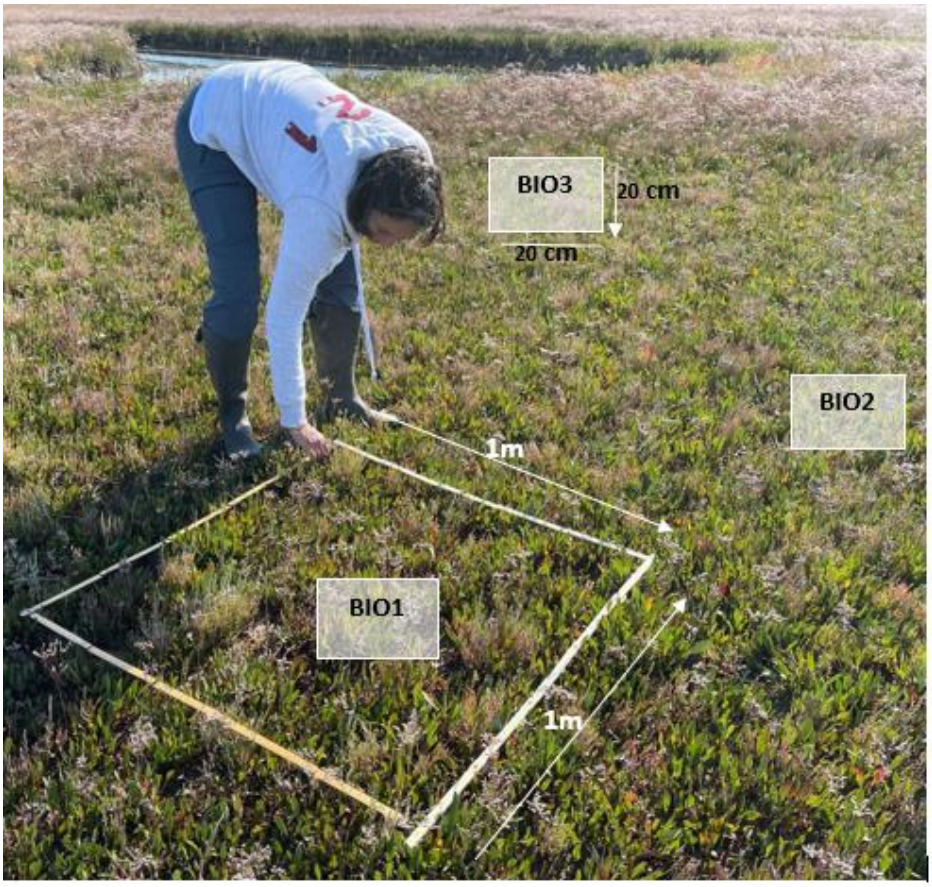

Figure 2-2 Area of plot and bio samples on the fiels using 1mx1m and 20cm x 20cm square rulers

Samples were collected in September 2021 at San Felice saltmarsh following the protocol by (Kristensen and Andersen, 1987). The field survey aimed to collecting aboveground vegetation and soil samples as well as belowground vegetation. The samples were collected in 10 different locations within the salt marsh. These sampling sites were referred to as “plots” and it was delimited by a 1m x1m square ruler. Each plot had 3 random replicates delimited by 20cm x 20cm square ruler referred as bio. The replicates also sampled the above-ground vegetation, below-ground (soil+roots), and soil. In total 30 sediment cores were collected from 10 plot sites as shown in the figure.

2.2.1 Aboveground vegetation

Above ground vegetation was collected using a knife, cutting the vegetation falling within the 20cmx20cm bios from the ground level and preserving the length of the plants, and then storing the vegetation in plastic bags before transport to the laboratory as shown in Figure 2-3.

Figure 2-3 – Aboveground vegetation sampling.

2.1.1 Soil+roots cores

Moreover, two different cylindrical PCV tubes were used to vertically inserted down the sediment and collect the sediment core to sample the below-ground (soil+roots) samples. Specifically, for the soil+roots sample we initially collected cores using a 10cm diameter and 10cm length cylindrical PVC tube which was vertically inserted down into the sediment, cutting through the roots, then partially digging around the tube with a spade to facilitate the safe removal of the soil core. This procedure was used only for the first four plots, because afterwards we decided to collect longer soil+roots cores. Therefore, the remaining six plots were sampled using an 8cm diameter and 30 cm length cylindrical PVC tube (Fig. 2-5). For each sample, the soil+roots core was immediately removed from the cylindrical tubes and manually measured with a ruler then sliced every 10 centimeters (this applied for the last six plots with the 30cm stratigraphic layer core). The slices were placed in properly labeled plastic bags (plot site with replicate reference + type of sample and depth if necessary), taken to the lab and then stored in a freezer before further laboratory process.

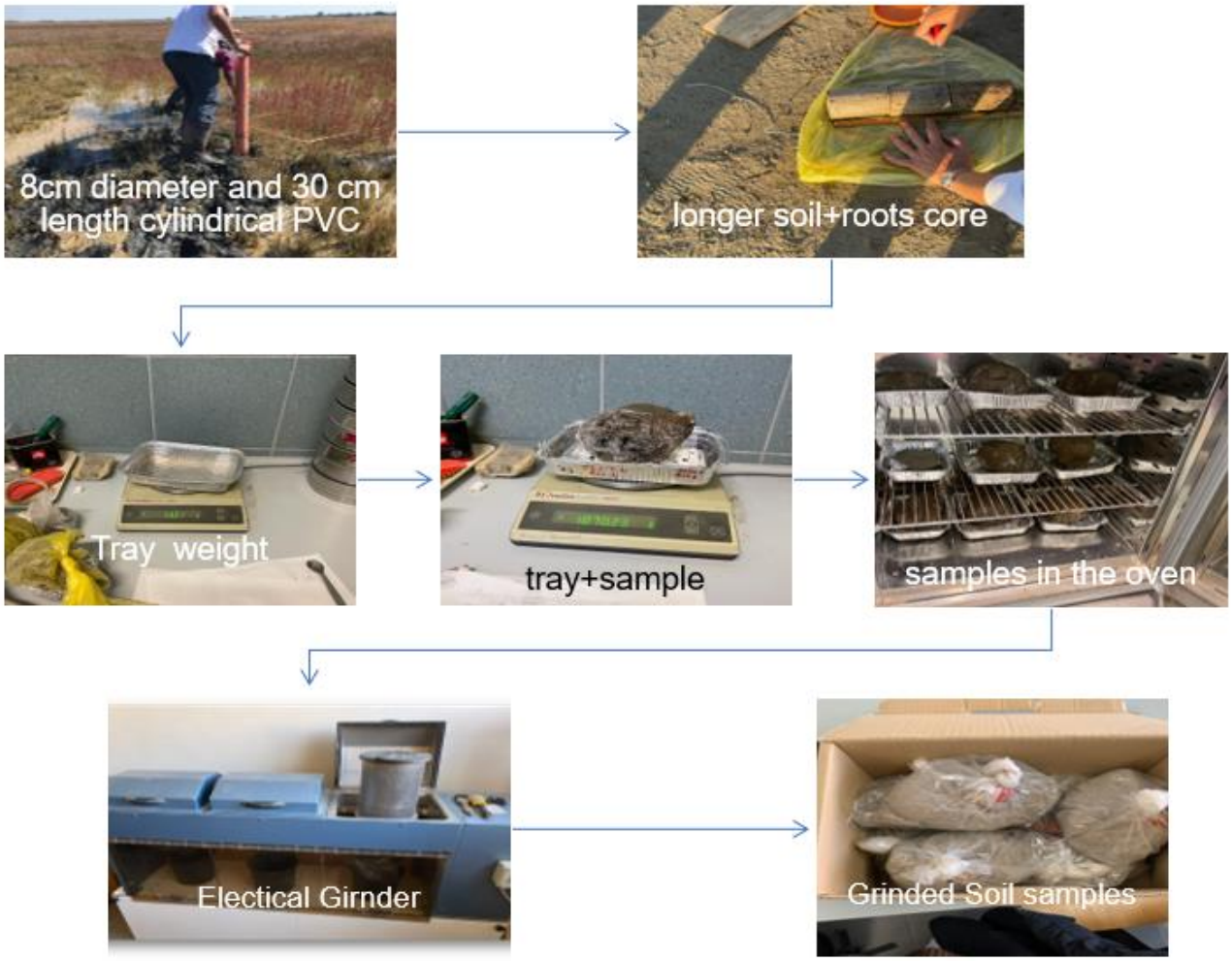

Figure 2-4 field and laboratory processes of below ground samples

Figure 2-5 Change in the PCV tube

2.3 Laboratory analyses

2.3.1. Aboveground vegetation

In the laboratory, the aboveground vegetation samples were put in paper bags, and weighed before and after dried (Fig. 2-6). During the drying process, the weight of the samples was controlled twice a day to monitor and ensure its stability: the samples were considered fully dried if the weight values were comparably the same the previous ones. The accepted difference from the previous weight was 0.5g. In general, the leaves and branches were oven-dried at a temperature of 70 °C for 72 hours.

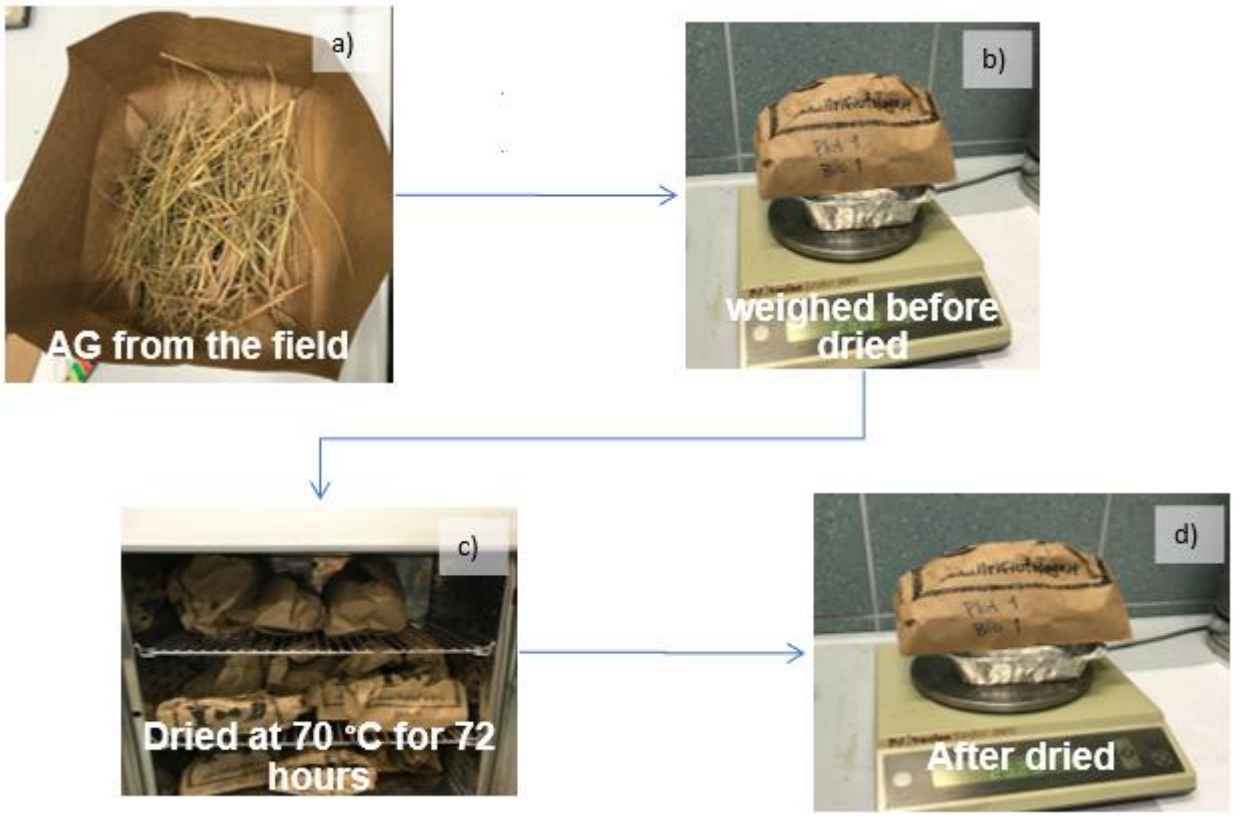

Figure 2-6 Laboratory process for the above ground biomass

2.3.2. Soil+roots cores

As shown in Fig. 2-7, after collecting the data from the field, (a) the samples were kept in a freezer to avoid decomposition. When ready to be processed, (b) the vegetation below-ground biomass was thawed from the freezer and then the samples were (c) placed two different steel sieves of 500 and 1000mm that were used simultaneously to allow the fine sediments and the below ground vegetation to remain on the sieves when washed (d). After (e) washing out the sediments from the sample, and the below ground vegetation (roots) were retained on the sieve, probably including a small portion of the finest particles

of sediments. A foil tray (f) was weighed before and after (g) placing the washed samples. The remaining material was put in the oven (h) at a temperature of 70° for 72 hours to determine the dry weight which was obtained after the samples were removed and weighed again (i) as the flowchart in Fig. 2-7 illustrates.

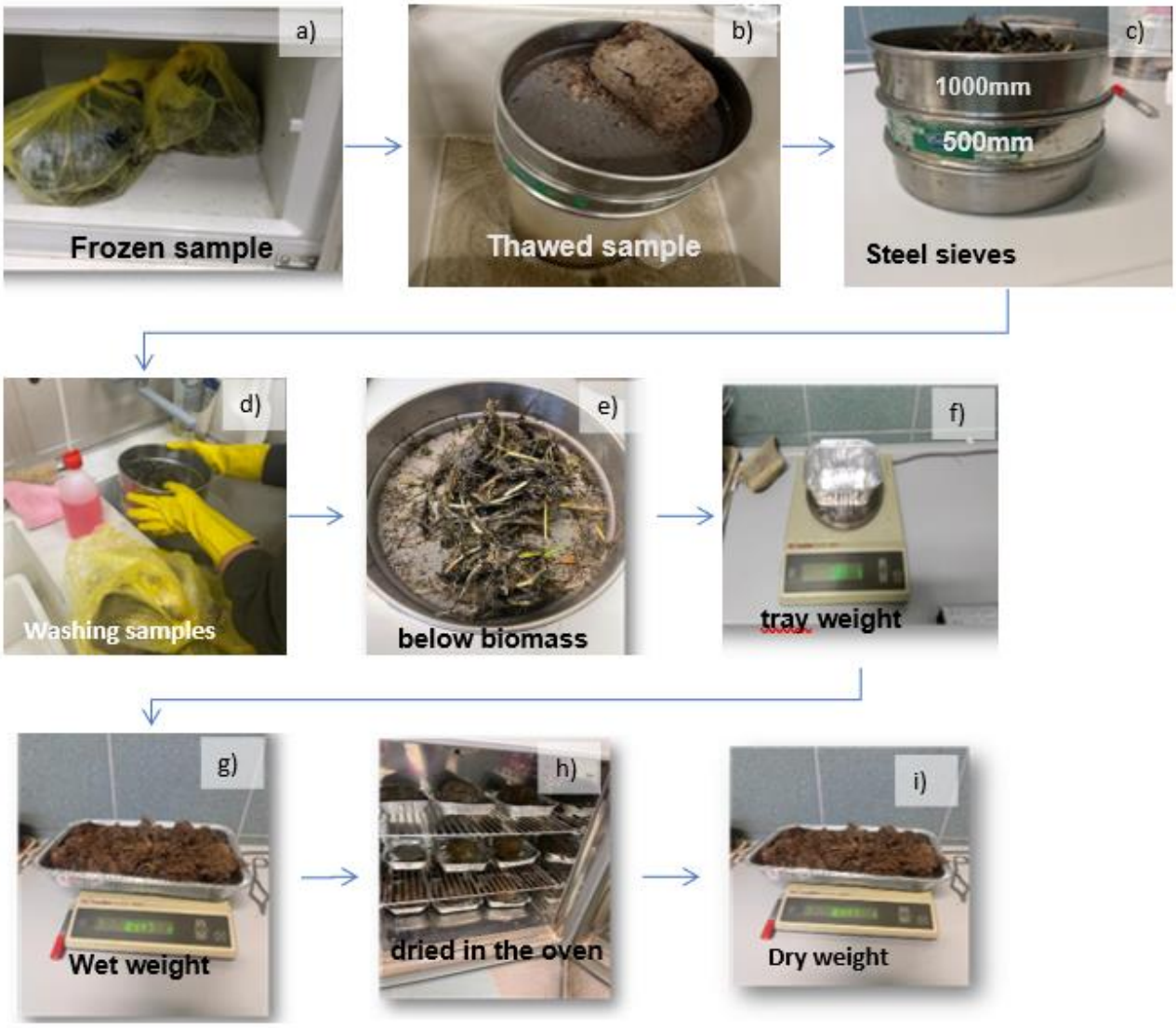

Figure 2-7 Laboratory processes of soil samples

2.3.3. Soil cores

To study a possible site-specific correlation between vegetation biomass and soil organic matter content the method of bulk density calculation and LOI was used. To initiate the process, sediment samples were removed from the freezer, the weight of empty aluminum trays was recorded and the samples were placed in the trays, put in the oven, dried at 105° C for 72 hours, controlling the weight twice a day (similar to the steps used for below ground biomass). To ensure the total dryness of the sediment cores, the samples were

only removed from the oven if the weight values were stable. The accepted difference from the previous weight was of 0.5.g. When dried, the weight of the tray was subtracted from the total weight (tray +sample) to obtain the value of the soil alone. When this was achieved, the samples weights (g) were used to calculate the dry bulk density (g cm-3) with the following equation:

$$3.\ Dry\ Bulk\ Density\ (g\ cm{-}3) = \frac{\text{Sediment Weight (g)}}{\text{Sediment Volume (cm3)}}$$

The soil samples were ground and processed again to obtain the bulk density and organic matter analysis through the Loss on Ignition (LOI) method.

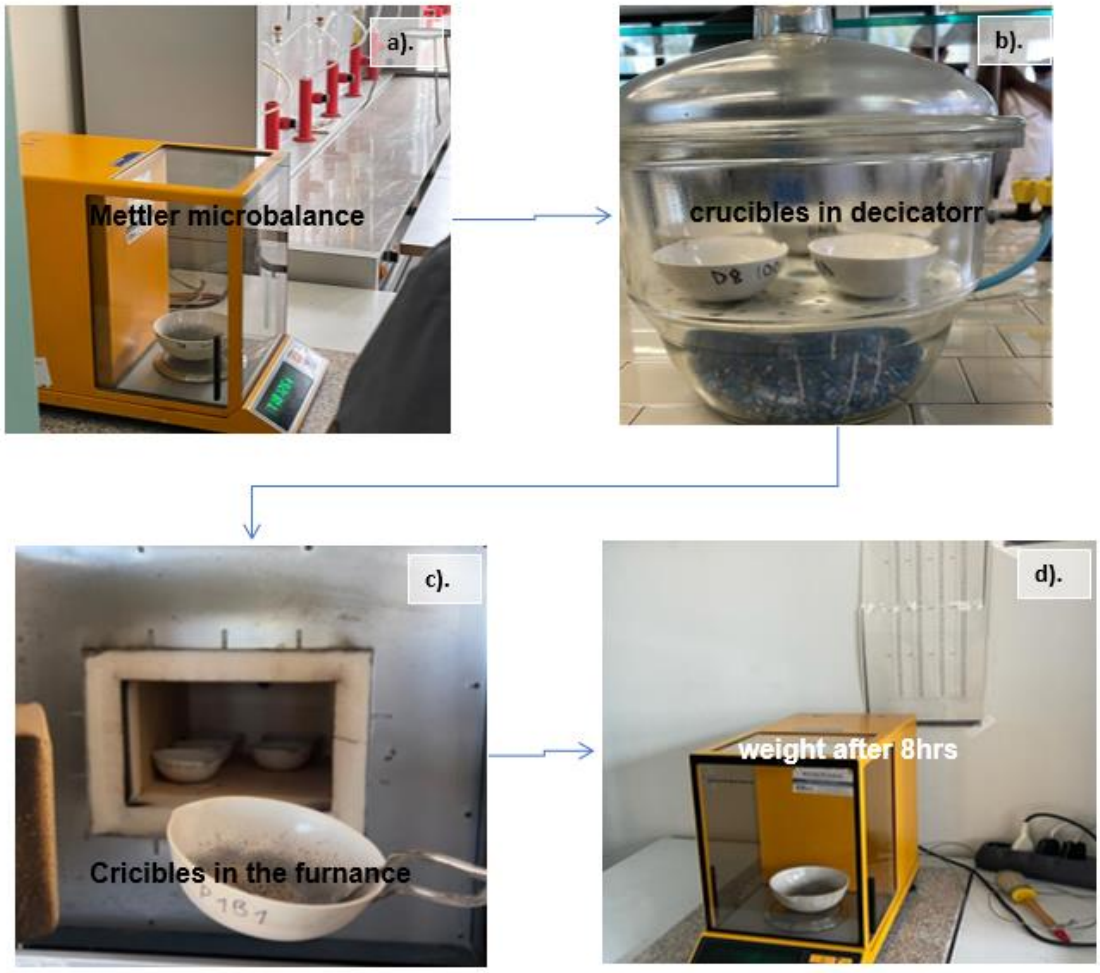

Figure 2-8 – The LOI process

Initially crucibles were washed with acid and dried in the oven. When dried, a). a Mettler microbalance of the model TECNOPOUND was used to obtain third decimal places weights of the dried crucibles. In each crucible 5-8g were added with the use of a laboratory spoon. b). The subsamples were left it in a desiccator for 30 min. After this the samples were quickly, weigh and record the exact weight of the crucible + sample to third decimal places. The crucibles c). were arranged in the furnace and the temperature was gradually by a temperature ramp of 100° C every 1hrs to go up to 450 ° C and leave for 8 hrs. The following day, the samples were removed from the furnace and the weight's

consistency of the samples was guaranteed by transferring them into a desiccator to cool down, then recording the ashes' weights. The obtained weights used to calculate the organic carbon in the soil followed the following equations:

1. % Ashes $= \frac{ashes}{(organic+ashes)} * 100$

2. $LOI = 100 - Ashes$

3. % O.C $= \frac{LOI}{1.724}$

2.4 Aerial Imaging Field Methods

To organize the field survey, various factors had to be considered such as tidal conditions of the marsh, and the perfect weather conditions for the drone to be flown (no rain and no clouds). In this way, our field activities initiated very early in the day before the sun and the tides rose, and to allow all the sampling equipment to be prepared on time as the images show (fig. 2-9).

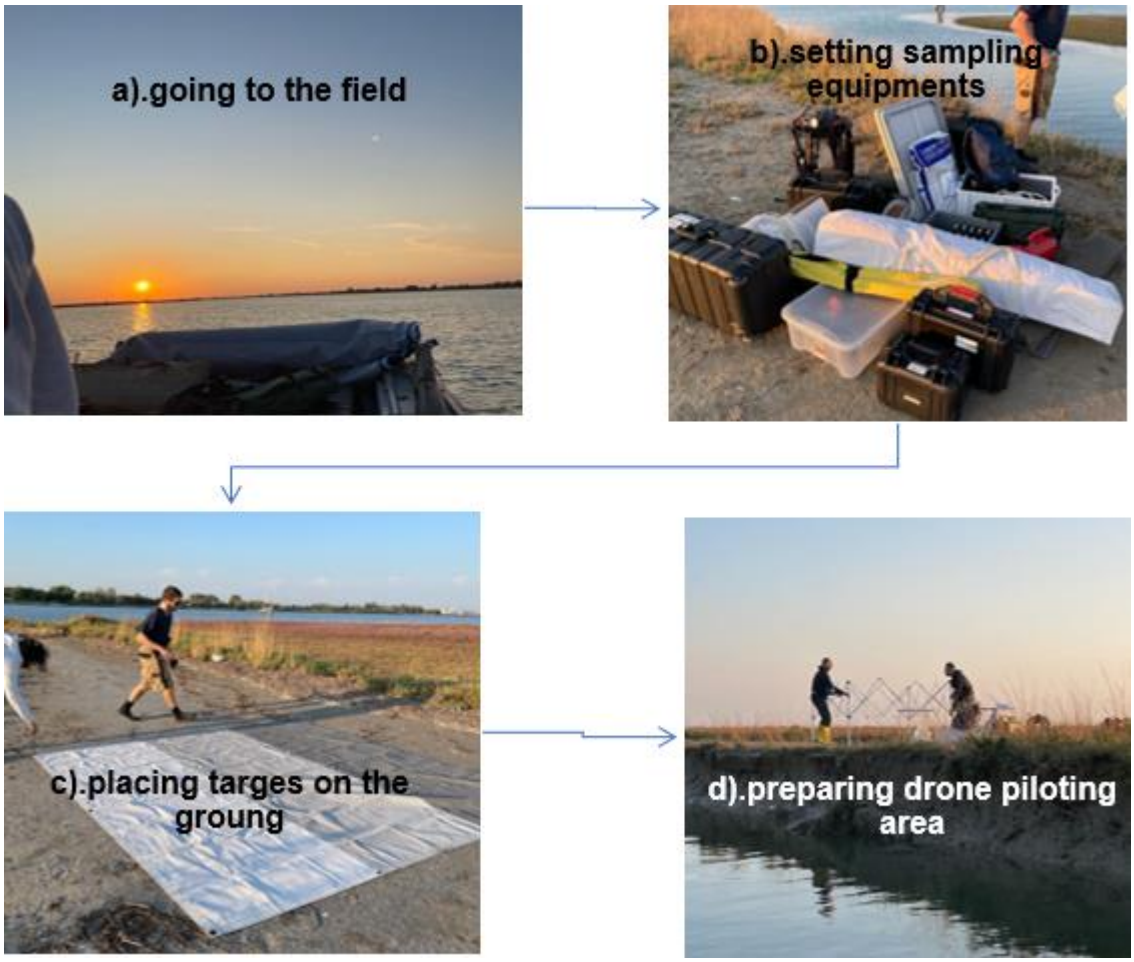

Figure 2-9 UAV flight preparation

The purpose was the collection of hyperspectral images to analyze the vegetation spatial distribution across the saltmarsh. The drone model used was a DJI Matrice 600 and it flew on September 8-10, 2021. The drone was equipped with a hyperspectral sensor Headwell Nano Hyperspec VNIR 273 that captured 270 contiguous spectral bands in the range 400-1000 nm. In the field, the first step was to place two targets on the ground that could be detected on the images. The radiance measured by the sensor on the targets was then used to calculate reflectance. To initiate the flight, the drone took several images of the calibration panel. The purpose of this process is to calibrate all the images that the sensor will capture. On the other hand, several ground control points (yellow targets) were fixed to the ground across the entire marsh. Taking the coordinates of where the targets were placed was vital to later georeference the images. The data set was pre-processed by the company (Archetipo s.r.l.) that performed the flight, which gave us the hyperspectral reflectance georeferenced product.

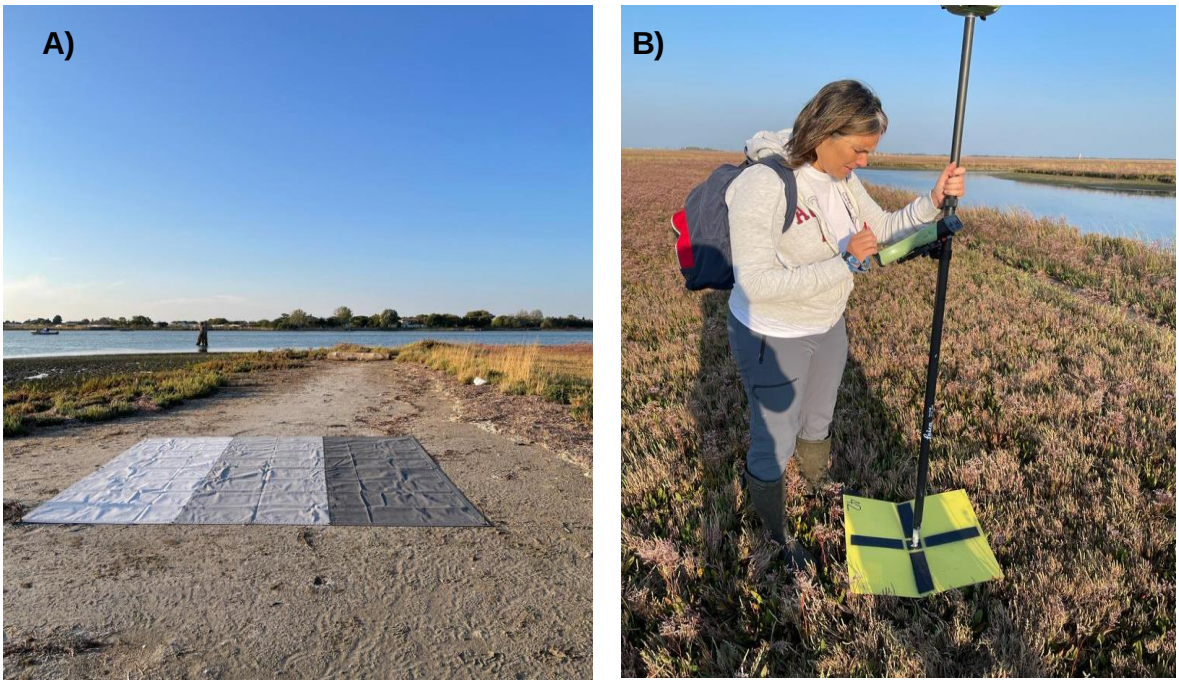

Figure 2-10. A) calibration control panels and B) GNSS measurement of the position of one ground control point.

2.5 Image Processing and Analysis

Data were processed using ENVI commercial software to obtain spectral reflectance of the different sampling sites, with the support of the GNSS points on the ground. The processing of these images required a sequence of operations such as building the spectral libraries of the different sampling areas by creating regions of interests (ROIs) for the different plots. The geographic coordinates that were used fell under WGS84 UTM ZONE 33N. These results were post-processed using Excel software to calculate the

different vegetation indexes and generate correlation graphs of the indices together with the obtained field results. Specifically, the hyperspectral reflectance recorded within the bands in the range 650 - 670 nm was averaged to calculate the reflectance of a RED band that mimics Landsat-9 and Sentinel 2. Similarly, the NIR band was mimicked .Similarly, the NIR band was calculated averaging the bands in the range 857 – 863 nm.

The RED and NIR bands for the different species associations were used along with the mean values for ABG and BGB to create correlation plots with the different indices (Appendix Table-2). To create the NDVI map, the ENVI band math tool was used to calculate the NDVI index based on bands 115-123 for the RED band and 208-215 for the NIR band.

Chapter 3

3. RESULTS

3.1. Results obtained from the analyses of field and laboratory data

The results obtained with the laboratory analyses have been reorganized based on the associations of halophytes sampled in the field. The 10 plots detected in the field were regrouped into 6 associations of halophytes characterized by the large majority of six species as described in Table 3-1, where the most abundant species and its percentage cover are coupled with the plot IDs.

Table 3-1. Name and percentage cover of the most abundant species in the associations of halophytes found within the 10 Plots.

Most abundant species	**Plot IDs**	**Percentage cover**
Inula crithmoides	Plot 10	≥ 50%
Sarcocornia fruticosa	Plot 8	≥ 80%
Liminium narbonense	Plot 1, Plot 2, Plot 5	≥ 80%
Spartina maritima	Plot 7	≥ 50%
Spartina anglica	Plot 4, Plot 6	≥ 90%
Salicornia veneta	Plot 3, Plot 9	≥ 40%

The average values of AGB, BGB, Bulk Density and LOI are shown in Table 3-2. We notice that if for BGB, Bulk Density and LOI, the values come exclusively from the Bios, as described in the Methods chapter, for the AGB we also used 25 samples randomly collected across the marsh in order to increase the accuracy of the estimate.

Table 3-2. AGB, BGB, Bulk Density and LOI for the associations of halophytes sampled in the field.

Most abundant species	**AGB (g/m2)**	**BGB (g/m2)**	**Bulk Denisty (g/cm3)**	**LOI (%)**
Inula crithmoides	897.7	3754.0	0.64	10.6
Sarcocornia fruticosa	1377.6	6392.7	0.49	13.6
Liminium narbonense	434.6	6319.7	0.49	15.0
Spartina maritima	424.9	4835.9	0.38	14.0
Spartina anglica	366.2	2041.7	0.46	10.8
Salicornia veneta	206.9	1552.3	0.46	9.4

Figure 3-1. shows a theoretical profile of the salt marsh (Silvestri et al. 2022) as well as the distribution of the AGB and BGB values. Figure 3.1 shows a theoretical profile of the

salt marsh (Silvestri et al. 2022) as well as the distribution of the AGB and BGB values. In the study site, the saltmarsh ranges between 0 cm and 40 cm of height. In general, *In.crit* and *Sar.fr* are found on the highest part of the marsh, *Lim.nar*. and *Sp.mar* are on the middle part of the marsh and *Sp.ang* and *Sal.ven* on the lowest part of the marsh. Therefore, the profile includes high-marsh species (i.e. *In.crit = Inula chritmoides; Sar. Fr. = Sarcoconia fruticosa*) that in general grow between 25/30 cm and 50 cm above mean sea level (a.m.s.l.), mid-marsh species (i.e. *Lim.nar. = Limonium narbonense; Sp.mar. = Spartina maritima*) that grow between 20 cm and 30 cm a.m.s.l., and low-marsh species (i.e. *Sp.ang. =Spartina anglica and Sal.ven. = Salicornia veneta*) that grow between 0 cm and 20 cm a.m.s.l. We notice that the species with the highest and lowest AGB production are *Sar.fr*. and *Sal. ven.,* with values of 6392.7 g/m2 and 206.9 g/m2 respectively. When BGB was compared, *Sal.ven* still is the lowest with values of 1552.3 g/m2, and *Sar.fr.* still has the highest value (639.3 g/m2). *In. crit*, Sar.fr, *Sp.ang* and *Sal.ven* have much larger AGB than BGB. In particular, *Sp. ang*., which is an invasive species that started to colonize the Venice lagoon saltmarshes about 10 years ago, has AGB more than twice the BGB. On the contrary, *Lim.nar* and *Sp. mar* have very similar AGB but their BGB differ, .*Lim.nar* (6319.7 g/m2). has a similar BGB to *Sar.fr.* (639.3 g/m2).

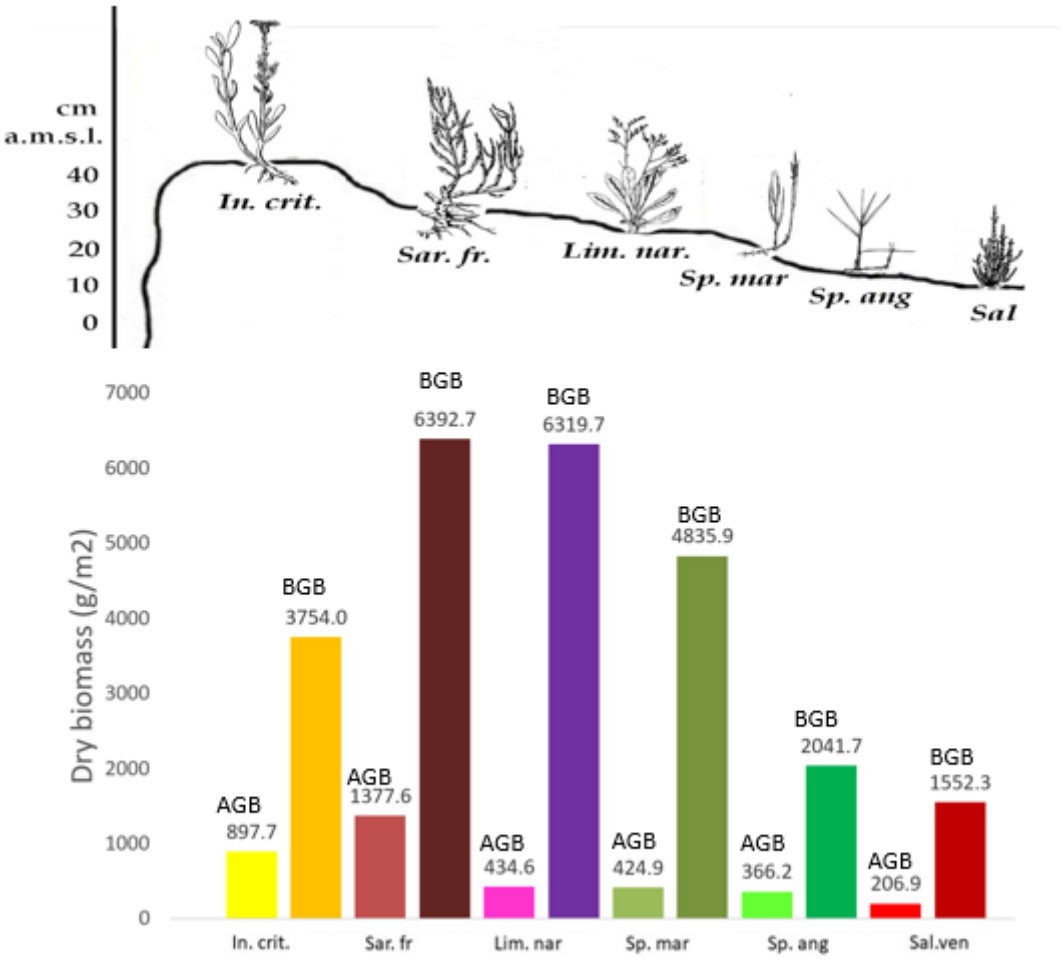

Figure 3-1. AGB and BGB retrieved from the analyses for the different associations of halophytes dominated by the six species*: In.crit = Inula crithmoides; Sar. Fr. = Sarcoconia*

fruticosa; Lim.nar. = Limonium narbonense; Sp.mar. = Spartina maritima; Sp.ang. =Spartina anglica and Sal.ven. = Salicornia veneta.

Figure 3.2 shows a positive correlation between the BGB and the AGB. The coefficient of determination R^2 is not very high probably because of the high discrepancy in the biomass production of the different species. However, a clear trend is visible. We can see that, in general, the BGB is about 4 times the AGB, event though with differences for some species. In fact, if this is true for *Sal.ven* and *Sp.ang*, the value increases for *Sp.mar*. and *Lim.nar*., that tend to have BGB of more than 5 times the AGB.

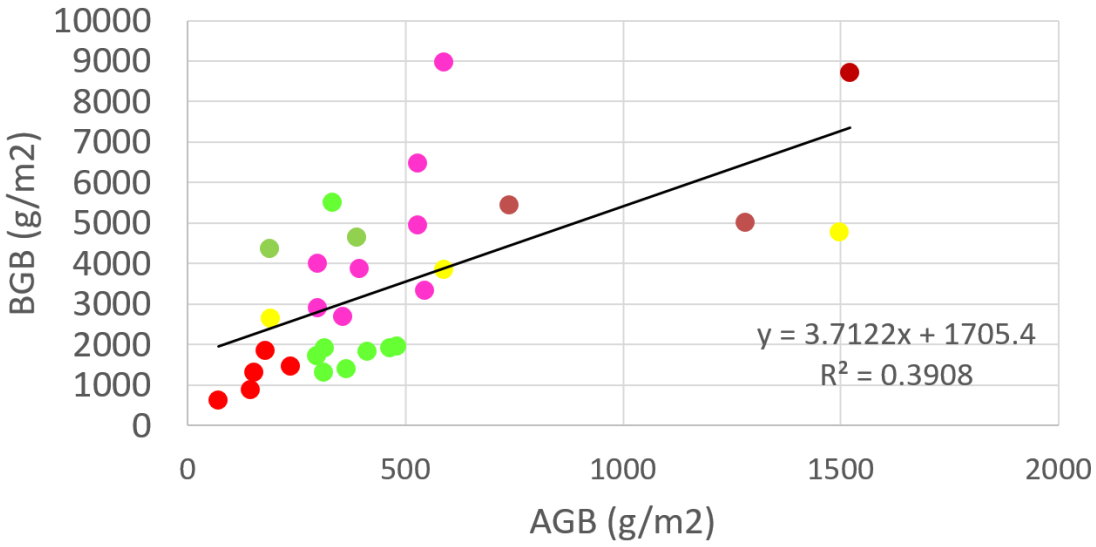

Figure 3-2. Below ground biomass (BGB) versus Above ground biomass (AGB)

Figure 3-3 shows that, in general, the BGB is mainly concentrated in the 0-10 cm depth range for all plant associations and decreases with depth. The highest BGB storage was found in the association dominated by *Lim. nar*, which accumulates more biomass than any other associations in the 0-10 cm and in the 10-20 cm ranges. On the contrary, *Sar.fr*. presents the second-highest BGB storage in the marsh, with a more evenly distributed balance across the three depth ranges. Other species such as *Sp.ang* and *Sal.ven*. show a limited amount of BGB in the top 0-10 cm and 10-20 cm layers, with a sharp decrease after the 20 cm of depth. On the other hand, even though *In.crit*. is on the high-marsh, it presents a very similar pattern as *Lim.nar*. Its AGB is limited, less than *Lim.nar* (Fig. 3-1), and the BGB is about half the amount of *Lim.nar*.

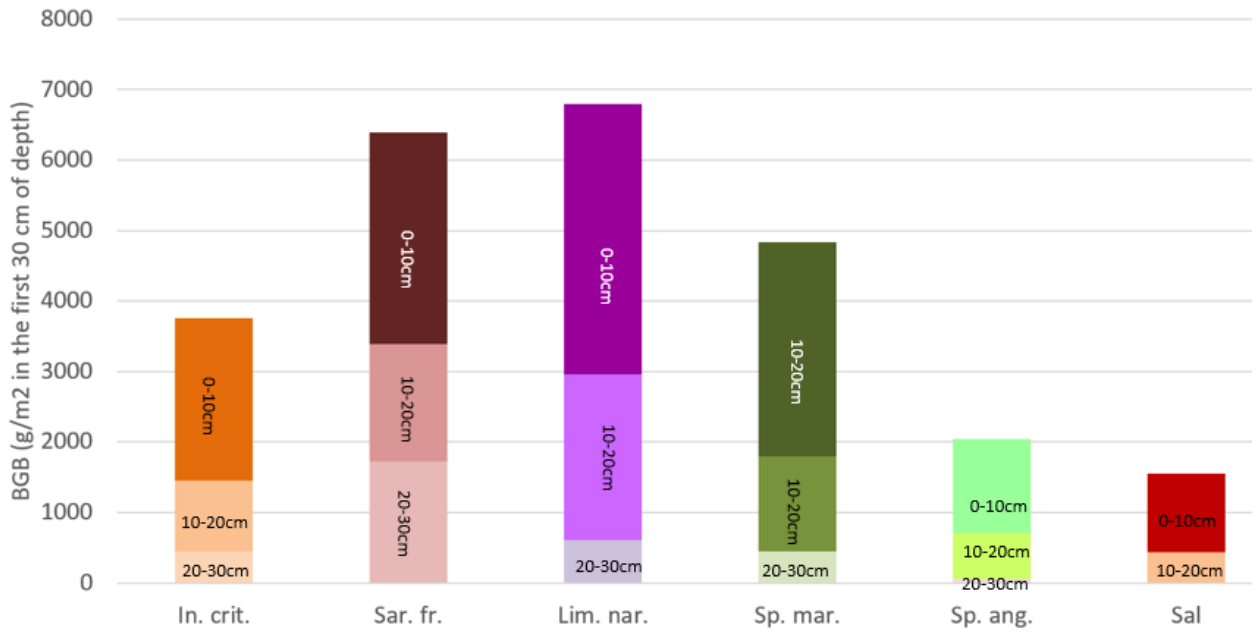

Figure 3-3. Values of below-ground biomass for the three depth ranges according to different species associations. The distribution of the BGB with depth is another interesting aspect.

The sum of AGB and BGB is presented in Figure 3-4. The greatest amount of total biomass is found in the high to middle part of the marsh, in fact *Sar.fr* contributes approximately 7500g/m2 of dry biomass if we consider AGB plus BGB, and *Lim.nar.* is the second contributor with more than 7200g/m2 total dry biomass. The high BGB attributed to *Sp.mar*. makes it the third in terms of total biomass, despite its very low AGB. The total biomass decreases moving from mid-marsh to low-marsh, with *Sal.ven* contributing a very small amount. In general, we notice that the total AGB+BGB value starts as low in the highest marsh portions, increases in the high-to-mid-marsh, then decreases again going towards the lower marsh portions.

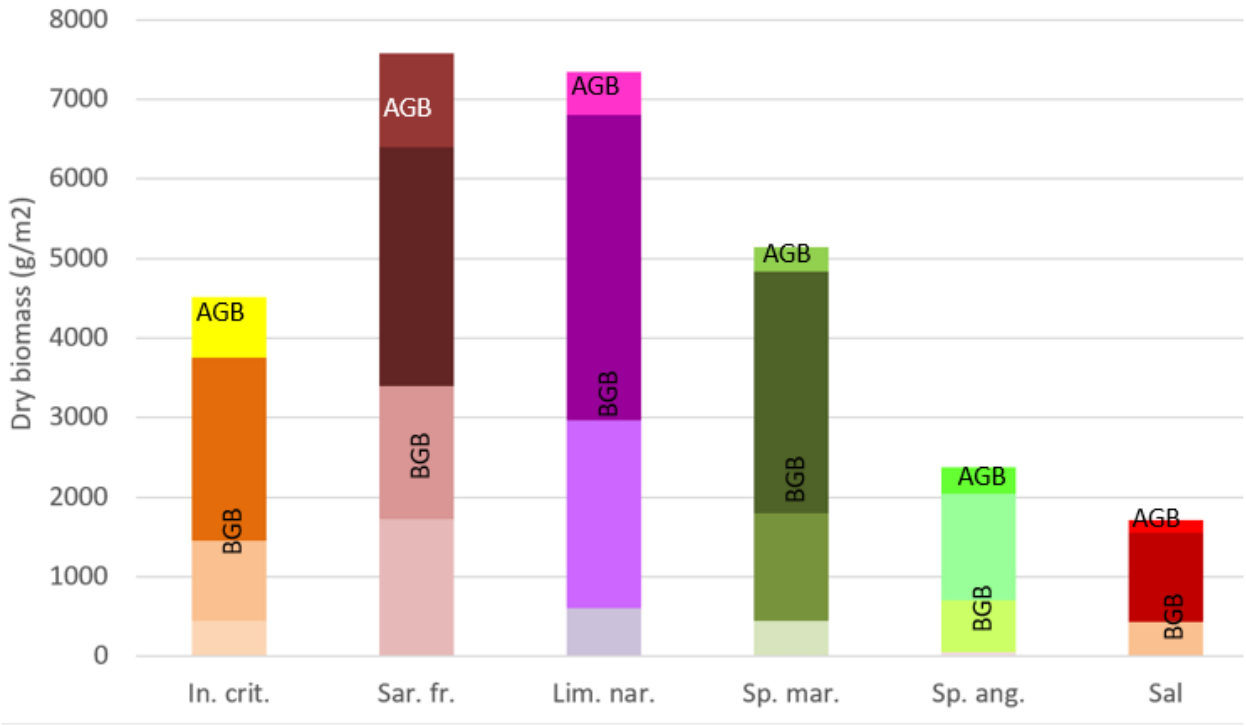

Figure 3-4. Values of below-ground biomass (BGB) according to different species association

The behavior is different when we look at the amount of organic matter that stays in the soil (Figure 3-4). Here in Figure3.5 the trend is favorable to the middle part of the marsh. The highest value of LOI is measured in the middle part of the marsh, with values ranging between 15% and 14% for *Lim.nar.* and *Sp.mar* respectively. The lowest values were measured in the lowest part of the marsh for *Sal.ven*. (LOI = 9.4%) and *Sp.ang*. (LOI = 10.8%). Similarly, in the high marsh, the values of LOI are also lower than in the mid-marsh, with Sar.fr. having LOI = 13.6% and *In.crit*. having LOI = 10.6%. In general, the difference between the values of LOI in the high, middle, and low varies significantly. The middle marsh presents the highest LOI values than any other part of the marsh. The high and the low marsh do not preserve greater amounts of organic matter in their soil.

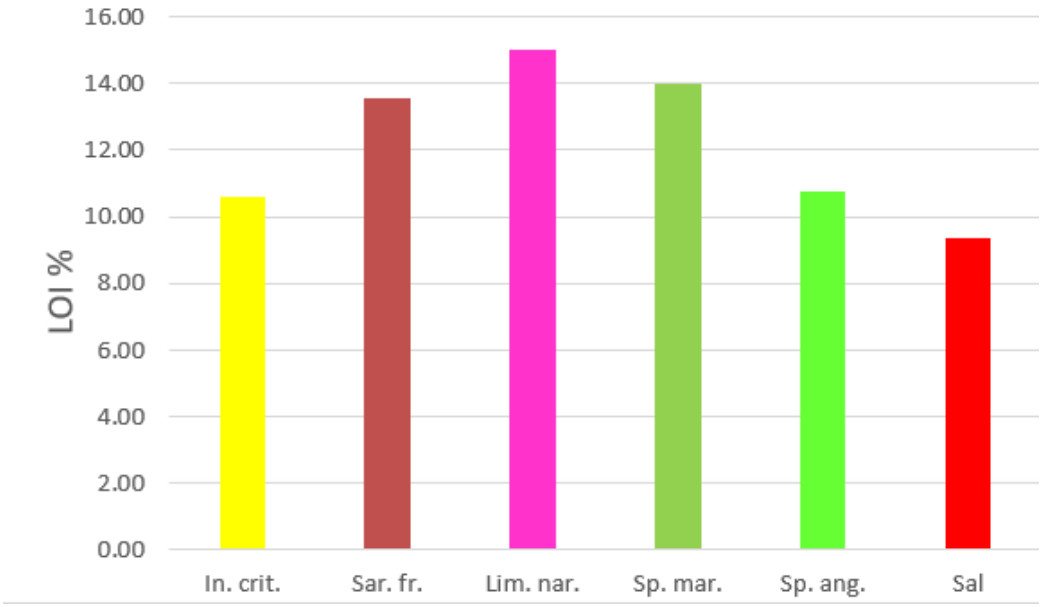

Figure 3-4. LOI for different vegetation associations

As for the Bulk Density, the results shown in Fig. 3-6 confirm that there is not a particular trend. Even though the BGB or the AGB increases for different associations, the Bulk Density ranges around 5000 g/cm^3, without showing any particular correlation with the two biomass variables. However, in general, the average bulk densities are lower for species such as *Sal.* and *Sp.ang.* The highest bulk density was observed for the species association dominated by *In.cri*.

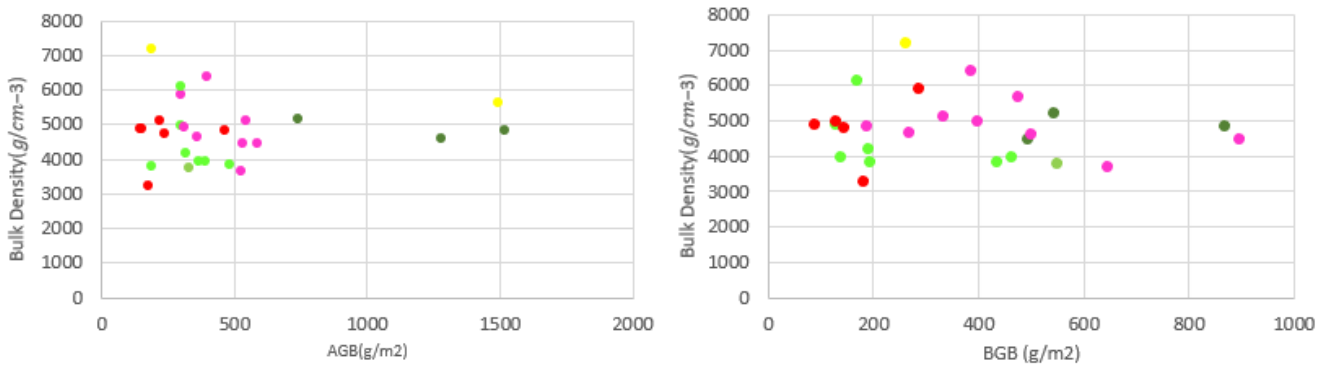

Figure 3-5. Comparison of the relationship between Bulk density versus Above ground biomass (AGB) and Bulk density versus Below ground biomass (BGB).

3.2. Results obtained from the analyses of hyperspectral data

The vegetation indices extracted from the average reflectance spectra of the pixels falling within the 10 Plots are analysed and correlated to AGB and BGB values.

Figure 3-7 shows the four indices selected for this thesis and correlate their values to the AGB vegetation amount determined in the lab. The indices range from 0 to 1. NDVI shows a high positive linear correlation with the AGB for values below 500 g/m^2. For values higher than this threshold, NDVI does not change, becoming stable at around 0.6 - 0.7. This means that the index becomes saturated. From Fig. 3-7 we can see that such behaviour interests *In.crit.* and *Sar.fr,* the associations that develop on the high-marsh and close to the channels. This is problematic because also *Lim.nar* and one of the *Sp.ang.* values fall at NDVI around 0.7, and therefore we must set a threshold not higher than 0.6 as the max NDVI value that allows a good correlation with the AGB, corresponding to AGB = 400 g/m^2.

In general, the correlation of other indices with AGB is weak. In all cases, the highest index values were observed for *Sar.fr*., while the lowest value was observed for *Sal.ven.* SAVI is probably the one index that best correlates to the AGB, however no vegetation index among those that were calculated performed well.

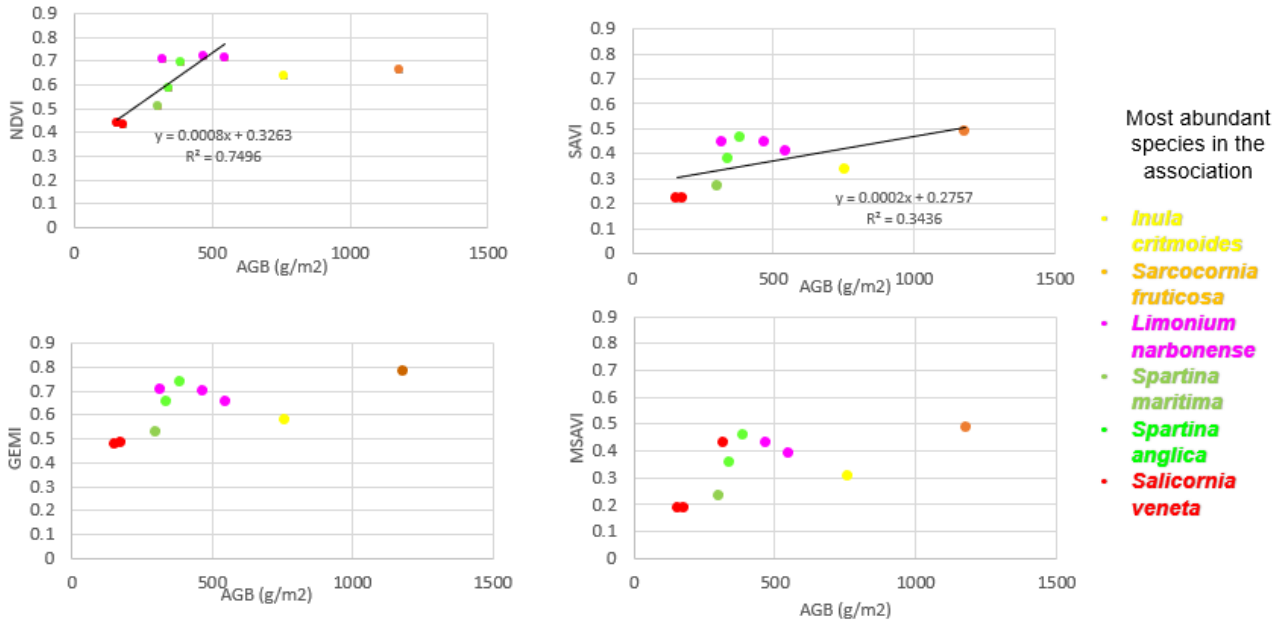

Figure 3-6. Values of the NDVI, SAVI, MSAVI, and GEMI indices for different above-ground biomass (AGB) measurements.

Fig. 3-8 plots the values of the considered vegetation indices versus the BGB. In all cases, the correlation is weak. The lowest values are still observed for *Sal.ven*., however, the highest NDVI value was observed for *Lim.nar.,* which is not the association with the highest BGB. *Inu.cr and Sar.fr* present high values of NDVI (0.6), although the BGB

values are low. All the species with low BGB had a high NDVI value. The other indices also have a negligible correlation with values of BGB.

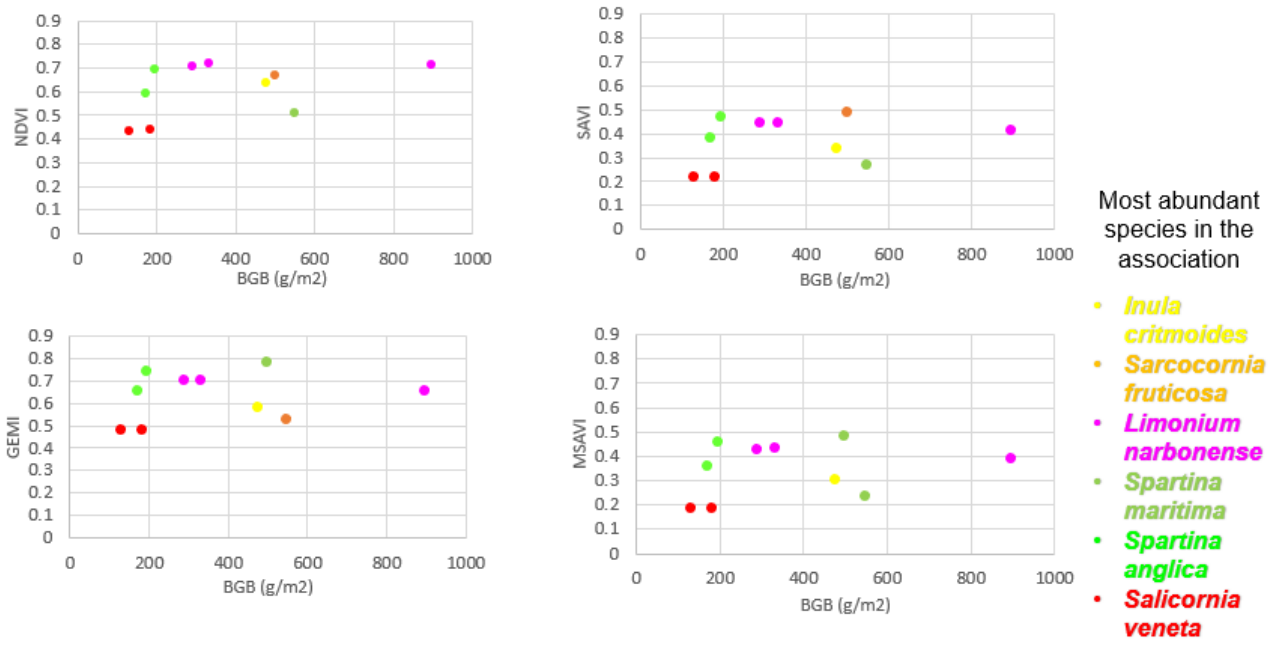

Figure 3-7. Values of the NDVI, SAVI, MSAVI, and GEMI indices for different below-ground biomass (BGB) measurements.

The NDVI values extracted across the study site from the hyperspectral images are shown in Fig. 3-9. Different colours attributed to the NDVI give us an indication of the distribution of the AGB across the marsh. We notice that most of the marsh is characterized by NDVI values larger than 0.6, which is the threshold above which the signal saturates and corresponds to AGB larger than 400 g/m^2 (red areas in Fig. 3-9). Only small portions of the inner marsh present NDVI values lower than 0.6, corresponding to AGB smaller than 400 g/m^2, and within the range 0.6 – 0.3 we see that the biomass decreases moving towards the ponded areas (going from green to yellow and to blue respectively – Fig. 3-9). These results indicate that most of the studied marsh is covered by dense vegetation, with AGB biomass larger than 400 g/m^2. Even though the number of data obtained with this work is limited, it gives a clear indication on the NDVI saturation effects as well as on the AGB distribution over the marsh. Other methods must be explored and combined with the hyperspectral data analysis to increase the accuracy and precision in the detection of the the AGB distribution across the marsh.

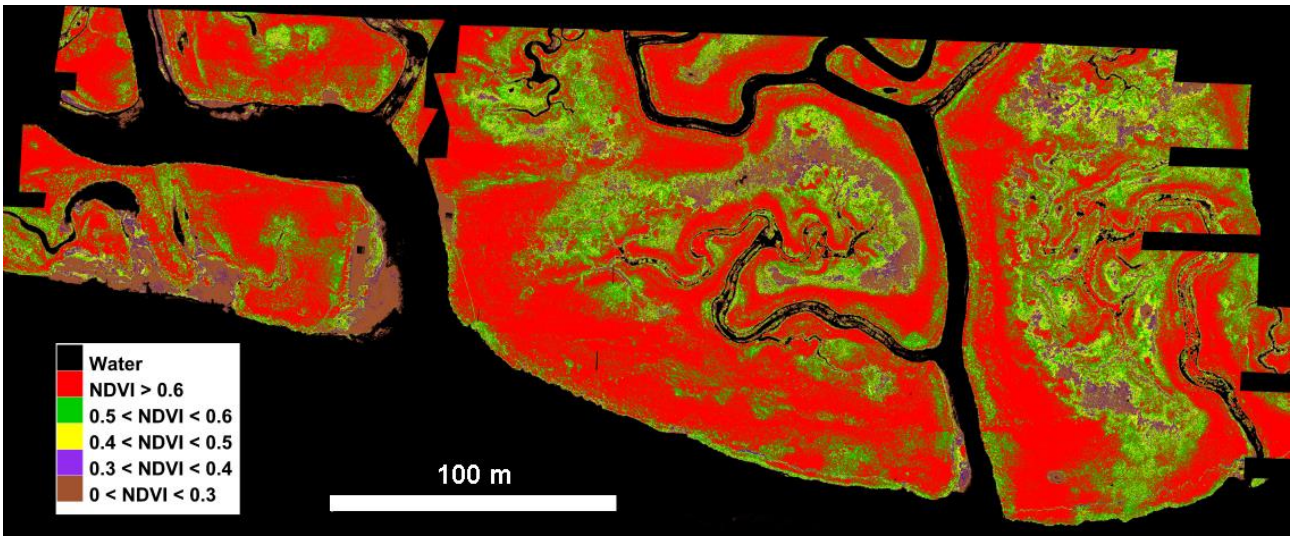

Figure 3-8. NDVI ranges across the study site.

Chapter 4

4. DISCUSSION AND CONCLUSIONS

ABOVEGROUND AND BELOWGROUND BIOMASS OF HALOPHYTES

As introduced in the first chapter, several authors (Krause et al.; Silvestri and Marani, 2004; Yang et al., 2020) proposed that tidal marshes receive more inorganic coarse sediments along the edges of the tidal creeks. This is because, when the tide enters the basin, the currents bring sediments along the channels and the creeks, therefore most of the sediments are trapped and deposited along the creeks' edges when the tide floods the marsh. This process increases the height of the levees with respect to the inner parts of the marsh, as we can see in the marsh profile of **Fig. 3.1**. Levees are usually colonized by vegetation species as *In. crit.* and *Sar. fr*. On the contrary, fine sediment inputs are important to the inner parts of the marsh, as they are situated at a lower elevation relative to the mean sea level, thus having a higher tidal inundation frequency, and consequently a higher rate of suspended sediment supply and deposition. These factors enhance the trapping of OM and fine sediment particles, increasing the saltmarsh's capacity for carbon burial (Duarte et al., 2005).

Another important factor in the carbon burial process is the presence and growth of vegetation. The largest store of carbon in coastal habitats is found within the soils. Carbon is primarily stored in aboveground and belowground biomass and then, thanks to the typical hypoxic conditions, is stored in soils. (Brevik and Homburg, 2004) suggests that C sequestration within a depositional environment is strongly related to biomass production. For C to be sequestered there must be biomass that is being produced in the area which will consequently be buried at the end of its cycle. We know that in general plants produce aboveground and belowground biomass. When the canopy or part of it dies, the aboveground material is deposited on the surface below the canopy; however, in tidal marshes there are several processes that contribute to export the deposited material, such tides, storm waves, wind. Therefore, the amount of organic matter coming from the aboveground parts of the canopy and that contributes to the marsh growth is very limited. On the contrary, the canopy belowground production and storage is very large for two main reasons: 1) roots and shoots cannot be exported by tides or wind; 2) the hypoxic conditions greatly reduce the decomposition of the OM. Both these factors are strongly linked to the position and distance to the creek network, because of the different hydrologic conditions that we find across the marsh.

In addition to these aspects, we must consider that several different species grow on tidal marshes, and they tend to create typical associations. For this reason, in this thesis we selected associations as main targets of the study, and each association is characterised by the large dominance of one species, as described in **Table 1**. (Silvestri and Marani, 2004) found that the zonation of various species respond differently to edaphic factors. This accounts for the species zonation that exists in the marsh. For example, *Sal.ven*. achieves its maximum biomass production in saline conditions, in the lower part of the

marsh were the tidal factors influence the most (see marsh profile in **Fig. 3.1**). On the other hand, *Spartina maritima* occurs at sites with strong reducing conditions, where other species, which are not sulphide-tolerant, cannot tolerate (Silvestri and Marani, 2004). While other species like *In.crit*. occurs along the edges of creeks and channels (Fig. 3.1), where both the hydraulic conductivity and the soil level in relation to the water table is high. In such areas the water availability, promotes aerobic conditions for roots to be degraded (Ursino et al., 2004). Moving from these considerations, in this thesis, the two main factors considered to properly understand the carbon burial trends, are the aboveground vegetation and the belowground vegetation in the layer 0-30 cm. The spatial distribution of different plant associations is also considered, to account for the spatial variability of edaphic factors and hydrological conditions.

Looking at the values retrieved from AGB and BGB analyses for the different associations of halophytes in **Figure 3.1**, we notice that the species that grow in the high and mid marsh, closer to the creeks, produce larger AGB and BGB than species that grow in the low marsh. *Sar.fr*. has the largest BGB (6392.7g/m2) but has the second smallest values of AGB (434.6g/m2). The second highest BGB belongs to *Lim.nar.* (6320 g/m2) which is the largest biomass producer of the mid marsh. As for the low marsh species, a study by (Willemsen et al., 2022) with feedback models between hydrodynamics, morphodynamics and vegetation dynamics found that salt marsh vegetation respond differently to different wave forcing. Medium waves contribute to the decrease of the width and height of the marsh in a way that the vegetation species can hardly germinate at lower elevations (Hs= 0.10 m), within the marsh. This supports our interpretation that the *Sal.ven* which is situated at 10 cm a.m.s.l. is the species that least produced both AGB and BGB in the entire marsh.

If we look at the distribution of BGB with depth for the different plant associations (**Fig. 3.3**) we notice that in all cases the biomass decreases with depth. However, what is very interesting is that if for high- and mid-marsh associations roots and shoots go down to 30 cm of depth, for low-marsh species almost all the biomass is found in the 0-20 cm layer, suggesting that the waterlogging is too high for the plants to develop tissues deeper than 20 cm from the soil surface. This is in agreement with (Ursino et al., 2004) that states that channels also acts as drainage and recharge zones, and they create favorable oxygenated soils where possibly plants have the ability to grow due to the sediments depositions. This is the case of *In.crit* in the Venice saltmarsh, while *Sal.ven*. and *Sp.ang*. have more difficulties of growing and develop being in the low marsh and far from creeks.

If we look at the total amount of biomass (AGB + BGB) produced by the different associations (**Fig. 3.4**) we notice that *Sar.fr.* and *Lim.nar* have a very similar amount, which is over 7000 g/m2. This is impressive, also because the large majority belongs to the belowground biomass that is the primary contributor of the marsh growth, as we have seen. It is interesting to note that *Lim.nar*. is the association with the highest BGB (**Fig. 3.3 and 3.4**), and this is probably due to the influence of hydrological factors. In fact, in our analyses we did not distinguish between dead and alive roots and shoots, accounting for the BGB coming from all the plant tissues that we found in the belowground samples. This means that dead undecomposed material may play a big role in the outcomes of our analyses. As already said, *Lim.nar.* grows at lower elevations with respect to *Sar.fr*. or *In.crit*., thus OM decomposition is slow due to more pronounced hypoxic conditions. These considerations are confirmed by the comparison of **Figure 3.4** with **Figure 3.5**, which

shows the behavior of the LOI (%) for the different associations. The effect of the local difference in the hydro-geomorphology of the sites plays a clear role in such comparison. The LOI retrieved for the middle part of the marsh is greater than for the higher and the lower part of the marsh. In the mid marsh, we observe the highest values of LOI reaching up to 15% as compared to the rest of the marsh. The lower LOI values in the high marsh could imply oxidized conditions that occur due to their positions near the edges of creeks and channels, where both the tidal range and the soil level with respect to the water table are higher (Silvestri and Marani, 2004). The vegetation that grows on the high marsh produces lots of biomass due to frequent sediment supply from tidal regimes, however, this biomass accumulation is decreased by the high decomposition rate due to the oxygen that infiltrates the soil and oxidizes the biomass in the soil. Therefore, high marsh species as *In.crit*. and *Sar.fr.* show high values of BGB but limited LOI values if compared to the mid-marsh association *Lim.nar*., that instead shows very high BGB as well as LOI values. The more hypoxic conditions typical of the mid-marsh preserve both the BGB (as seen in **Fig. 3.4**) and increase the organic matter in the soil, as shown by the LOI values (**Fig. 3.5**).

Another important result comes from the comparison of the AGB with the BGB retrieved in this study (**Fig. 3.2**). The fact that in general, the BGB increases linearly with the AGB seams trivial, but it is not. First, we notice that this behaviour is general, i.e. includes all the associations that were sampled in the field. Even though the determination coefficient is not very high (R^2 = 0.4), the generality of this relation is extremely valuable. I mean that whenever we see or measure a large AGB value on the marsh surface, we are confident that the BGB accumulated underneath is large too. And considering the amount of work and time needed to retrieve the BGB in the field and in the lab, the relation is even more noticeable. This relation is also the key link to the use of remote sensing in this thesis. In fact, remote sensing can be used to retrieve spectral signals that allow us to calculate vegetation indices (VIs). Since we have seen that VIs are good proxies of AGB, we can use them to infer the spatial distribution of the AGB across the marsh. This is a big step forward if we consider that field campaigns are extremely time consuming and allow the collection of a small number of samples. Therefore, UAV systems, as the one used in this study, allow determining the spatial distribution of the selected VI, which can be calibrated using limited field observations, as we performed in this research. Since the VIs can be used to infer only the AGB, as we just said, a significant correlation between AGB and BGB allows us to make predictions about the BGB, which is a quantity that could not be measured from remote sensing otherwise.

In this work, four vegetation indices were selected, and their values calculated to provide a spatial representation of vegetation variability throughout the marsh. The potential correlation of the four different indices with AGB and BGB values was also evaluated (Figure 3-7 and Figure 3-8). When analyzing the correlation between the indices and the ABG values, it is noticeable that NDVI and SAVI perform better than GEMI and MSAVI. However, NDVI represented vegetation with AGB in the lower and middle parts of the marsh (Lim.nar) better than all other indices and showed a strong linear positive correlation (Fig. 3-7). The values of AGB in this region are not very high, indicating that NDVI is a good proxy in the low and middle marsh areas. In areas where the AGB is high (Sar.fr. and In.crit.), the index becomes saturated. A possible explanation for this could be that the NDVI is sensitive to saturation problems in dense canopies (Swoish et al., 2022). None of the other indices calculated in this work provided better results. The SAVI index,

for example, is known to separate vegetation from the soil factor. Our results show a very low correlation of SAVI with AGB in salt marsh. The soil factor in salt marsh is low because species continue to compete for space to grow and tend to colonize the surface of the interstitial space. This phenomenon could be a possible explanation for why SAVI values were poorly correlated with AGB. The MSAVI index was developed to improve the SAVI index. Therefore, the MSAVI also has lower values.

The relationship between the index values and the BGB was found to be weak. This analysis was performed even though it is known that vegetation indices were developed to study aboveground vegetation based on physical characteristics related to photosynthetic activity. However, since we found a significant correlation between AGB and BGB (Fig. 3.2), we also tested the correlation of vegetation indices with BGB. No clear correlations were found, which could be due to the limited amount of data available.

The final result of this thesis, i.e. the NDVI map shown in **Fig. 3-9**, suggests interesting insights on the biomass distribution across the studied saltmarsh. High NDVI values (NDVI > 0.6, i.e. red areas in **Fig. 3.9**) are located between the inner part of the marsh and the creeks, including the levees. Most of the marsh area belongs to this category, suggesting that the majority of the marsh has AGB larger than 400 g/m^2 (see **Fig. 3.7**). The areas with 0.3 < NDVI < 0.6 are located in the inner marsh portions, where small creeks end and create ponds and salt pans. These areas, usually colonized by *Sal.ven*. and *Sp. spp*. are the lowest portions of the marsh, difficult to colonize, and our results suggest that here the AGB is lower than 400 g/m2 (see **Fig. 3.7**). These low areas cover a small surface of the marsh if compared to the large areas colonized by mid- and high-marsh species, where the biomass is larger.

CONCLUSIONS

In conclusion, this study discussed approaches of quantifying the biomass distribution in a salt marsh of the Venice Lagoon. The analyses also focused on the amount of organic matter stored in soils. Hyperspectral data collected through a UAV system were used to compute vegetation indices to retrieve possible correlations to AGB and BGB. The results show that: (i) the species that grow in the high and mid marsh, closer to the creeks, produce larger AGB and BGB than species that grow in the low marsh; (ii) belowground, the vegetation biomass decreases with depth and low-marsh species (*Sal.ven*. and *Sp.ang*.) do not produce biomass below 20 cm from the soil surface; (iii) *Lim.nar*. is the association that contributes most to the biomass stored in the marsh soil as well as to the soil organic matter; (iv) in general, the BGB increases linearly with the AGB; (v) NDVI is a good proxy for the AGB only for low and mid-marsh vegetation species, while it saturates for high-marsh high-biomass vegetation; (vi) most of the studied marsh is covered by dense vegetation, with AGB biomass larger than 400 g/m^2.

REFERENCES

Adame, F., Lovelock, C., 2011. Carbon and nutrient exchange of mangrove forests with the coastal ocean. Hydrobiologia 663, 23–50. https://doi.org/10.1007/s10750-010-0554-7

Adame, M.F., Kauffman, J.B., Medina, I., Gamboa, J.N., Torres, O., Caamal, J.P., Reza, M., Herrera-Silveira, J.A., 2013. Carbon Stocks of Tropical Coastal Wetlands within the Karstic Landscape of the Mexican Caribbean. PLOS ONE 8, e56569. https://doi.org/10.1371/journal.pone.0056569

Alongi, D., 2014. Carbon Cycling and Storage in Mangrove Forests. Annual review of marine science 6, 195–219. https://doi.org/10.1146/annurev-marine-010213-135020

Alongi, D.M., 2020a. Carbon Balance in Salt Marsh and Mangrove Ecosystems: A Global Synthesis. Journal of Marine Science and Engineering 8, 767. https://doi.org/10.3390/jmse8100767

Alongi, D.M., 2020b. Carbon Balance in Salt Marsh and Mangrove Ecosystems: A Global Synthesis. Journal of Marine Science and Engineering 8, 767. https://doi.org/10.3390/jmse8100767

Barbier, E.B., Hacker, S.D., Kennedy, C., Koch, E.W., Stier, A.C., Silliman, B.R., 2011. The value of estuarine and coastal ecosystem services. Ecological Monographs 81, 169–193. https://doi.org/10.1890/10-1510.1

Bell, R.-A., Callow, J.N., 2020. Investigating Banksia Coastal Woodland Decline Using Multi-Temporal Remote Sensing and Field-Based Monitoring Techniques. Remote Sensing 12, 669. https://doi.org/10.3390/rs12040669

Best, U., Wegen, M., Dijkstra, J., Borsje, B.W., Willemsen, P., Roelvink, D.J.A., 2018. Do salt marshes survive sea level rise? Modelling wave action, morphodynamics and vegetation dynamics. Environmental Modelling and Software 109, 152–166. https://doi.org/10.1016/j.envsoft.2018.08.004

Blankespoor, B., Dasgupta, S., Laplante, B., 2014. Sea-level rise and coastal wetlands. Ambio 43, 996–1005. https://doi.org/10.1007/s13280-014-0500-4

Borsje, B.W., Wesenbeeck, B.K. van, Dekker, F., Paalvast, P., Bouma, J., Katwijk, M.M. van, Vries, M. de, 2011. How ecological engineering can serve in coastal protection. ECOL ENG 37, 113–122. https://doi.org/10.1016/j.ecoleng.2010.11.027

Bouma, T.J., Vries, M. de, Low, E., Peralta, G., Tánczos, I.C., Koppel, L. van, Herman, P.M.J., 2005. Trade-offs related to ecosystem engineering: a case study on stiffness of emerging macrophytes. ECOLOGY 86, 2187–2199. https://doi.org/10.1890/04-1588

Brevik, E.C., Homburg, J.A., 2004a. A 5000 year record of carbon sequestration from a coastal lagoon and wetland complex, Southern California, USA. CATENA 57, 221–232. https://doi.org/10.1016/j.catena.2003.12.001

Brevik, E.C., Homburg, J.A., 2004b. A 5000 year record of carbon sequestration from a coastal lagoon and wetland complex, Southern California, USA. CATENA 57, 221–232. https://doi.org/10.1016/j.catena.2003.12.001

Chapman, V.J., 1976. Coastal vegetation, second. ed. Elsevier, Pergamon Press, Oxford.

Chen, R., Twilley, R.R., 1999. A simulation model of organic matter and nutrient accumulation in mangrove wetland soils. Biogeochemistry 44, 93–118. https://doi.org/10.1007/BF00993000

Chmura, G.L., Anisfeld, S.C., Cahoon, D.R., Lynch, J.C., 2003. Global carbon sequestration in tidal, saline wetland soils. Global Biogeochemical Cycles 17. https://doi.org/10.1029/2002GB001917

Craft, C., 2007. Freshwater input structures soil properties, vertical accretion, and nutrient accumulation of Georgia and U.S tidal marshes. Limnology and Oceanography 52, 1220–1230. https://doi.org/10.4319/lo.2007.52.3.1220

Duarte, C.M., Middelburg, J.J., Caraco, N., 2005. Major role of marine vegetation on the oceanic carbon cycle 8.

Ellison, A.M., 1987. Effects of Competition, Disturbance, and Herbivory on Salicornia Europaea. Ecology 68, 576–586. https://doi.org/10.2307/1938463

Feagin, R., Lozada-Bernard, S., Ravens, T., Möller, I., Yeager, K., Baird, A., 2009. Does Vegetation Prevent Wave Erosion of Salt Marsh Edges? Proceedings of the National Academy of Sciences of the United States of America 106, 10109–13. https://doi.org/10.1073/pnas.0901297106

Feller, I., Lovelock, C., Berger, U., McKee, K., Joye, S., Ball, M., 2010. Biocomplexity in Mangrove Ecosystems. Annual review of marine science 2, 395–417. https://doi.org/10.1146/annurev.marine.010908.163809

Fourqurean, J.W., Duarte, C.M., Kennedy, H., Marbà, N., Holmer, M., Mateo, M.A., Apostolaki, E.T., Kendrick, G.A., Krause-Jensen, D., McGlathery, K.J., Serrano, O., 2012. Seagrass ecosystems as a globally significant carbon stock. Nature Geosci 5, 505–509. https://doi.org/10.1038/ngeo1477

Gacia, E., Duarte, C.M., 2001. Sediment Retention by a Mediterranean Posidonia oceanica Meadow: The Balance between Deposition and Resuspension. Estuarine, Coastal and Shelf Science 52, 505–514. https://doi.org/10.1006/ecss.2000.0753

Hodáňová, D., 1981. Plant strategies and vegetation processes. Biol Plant 23, 254–254. https://doi.org/10.1007/BF02895358

Huete, A.R., 1988. A soil-adjusted vegetation index (SAVI). Remote Sensing of Environment 25, 295–309. https://doi.org/10.1016/0034-4257(88)90106-X

IPCC, 2014. Climate Change 2014: Synthesis Report. Contribution of Working Groups I, II and III to the Fifth Assessment Report of the Intergovernmental Panel on Climate Change. IPCC, Geneva, Switzerlan.

Kelleway, J.J., Saintilan, N., Macreadie, P.I., Ralph, P.J., 2016. Sedimentary Factors are Key Predictors of Carbon Storage in SE Australian Saltmarshes. Ecosystems 19, 865–880. https://doi.org/10.1007/s10021-016-9972-3

Kennedy, H., Beggins, J., Duarte, C.M., Fourqurean, J.W., Holmer, M., Marbà, N., Middelburg, J.J., 2010. Seagrass sediments as a global carbon sink: Isotopic constraints. Global Biogeochemical Cycles 24. https://doi.org/10.1029/2010GB003848

Kirwan, M.L., Guntenspergen, G.R., D'Alpaos, A., Morris, J.T., Mudd, S.M., Temmerman, S., 2010. Limits on the adaptability of coastal marshes to rising sea level. Geophysical Research Letters 37. https://doi.org/10.1029/2010GL045489

Kirwan, M.L., Megonigal, J.P., 2013. Tidal wetland stability in the face of human impacts and sea-level rise. Nature 504, 53–60. https://doi.org/10.1038/nature12856

Kirwan, M.L., Temmerman, S., Skeehan, E.E., Guntenspergen, G.R., Fagherazzi, S., 2016. Overestimation of marsh vulnerability to sea level rise. Nature Clim Change 6, 253–260. https://doi.org/10.1038/nclimate2909

Klemas, V., R.Field, O.Weatherbee, 2003. Uses and limitations of remote sensing for coastal zone management.

Krause, J.R., Hinojosa-Corona, A., Gray, A.B., Herguera, J.C., McDonnell, J., Schaefer, M.V., Ying, S.C., Watson, E.B., 2022. Beyond habitat boundaries: Organic matter cycling requires a system-wide approach for accurate blue carbon accounting. Limnology and Oceanography n/a. https://doi.org/10.1002/lno.12071

Kristensen, E., Andersen, F.Ø., 1987. Determination of organic carbon in marine sediments: a comparison of two CHN-analyzer methods. Journal of Experimental

Marine Biology and Ecology 109, 15–23. https://doi.org/10.1016/0022-0981(87)90182-1
Kristensen, E., Bouillon, S., Dittmar, T., Marchand, C., 2008. Organic carbon dynamics in mangrove ecosystems: A review. Aquatic Botany, Mangrove Ecology – Applications in Forestry and Costal Zone Management 89, 201–219. https://doi.org/10.1016/j.aquabot.2007.12.005
Kusumaningtyas, M.A., Hutahaean, A.A., Fischer, H.W., Pérez-Mayo, M., Ransby, D., Jennerjahn, T.C., 2019. Variability in the organic carbon stocks, sources, and accumulation rates of Indonesian mangrove ecosystems. Estuarine, Coastal and Shelf Science 218, 310–323. https://doi.org/10.1016/j.ecss.2018.12.007
Lovelock, C., Duarte, C., 2019. Dimensions of Blue Carbon and emerging perspectives. Biology letters 15. https://doi.org/10.1098/rsbl.2018.0781
Lovelock, C.E., Adame, M.F., Bennion, V., Hayes, M., O'Mara, J., Reef, R., Santini, N.S., 2013. Contemporary Rates of Carbon Sequestration Through Vertical Accretion of Sediments in Mangrove Forests and Saltmarshes of South East Queensland, Australia. Estuaries and Coasts 37, 763–771. https://doi.org/10.1007/s12237-013-9702-4
Marani, M., Belluco, E., D'Alpaos, A., Defina, A., Lanzoni, S., Rinaldo, A., 2003. On the drainage density of tidal networks. Water Resources Research 39. https://doi.org/10.1029/2001WR001051
Mcleod, E., Chmura, G.L., Bouillon, S., Salm, R., Björk, M., Duarte, C.M., Lovelock, C.E., Schlesinger, W.H., Silliman, B.R., 2011. A blueprint for blue carbon: toward an improved understanding of the role of vegetated coastal habitats in sequestering CO2. Frontiers in Ecology and the Environment 9, 552–560. https://doi.org/10.1890/110004
Mitsch, W., Gosselink, J., 2000. The Value of Wetlands: Importance of Scale and Landscape Setting. Ecological Economics 35, 25–33. https://doi.org/10.1016/S0921-8009(00)00165-8
Mudd, S.M., Howell, S.M., Morris, J.T., 2009. Impact of dynamic feedbacks between sedimentation, sea-level rise, and biomass production on near-surface marsh stratigraphy and carbon accumulation. Estuarine, Coastal and Shelf Science 82, 377–389. https://doi.org/10.1016/j.ecss.2009.01.028
NSF, 2021. Coupled Ecological-Geomorphological Response of Coastal Wetlands to Environmental Change [WWW Document]. URL https://www.nsf.gov/awardsearch/showAward?AWD_ID=2016068&HistoricalAwards=false (accessed 6.29.22).
Owers, C.J., Rogers, K., Mazumder, D., Woodroffe, C.D., 2020. Temperate coastal wetland near-surface carbon storage: Spatial patterns and variability. Estuarine, Coastal and Shelf Science 235, 106584. https://doi.org/10.1016/j.ecss.2020.106584
Pethick, J., 1995. An Introduction to Coastal Geomorphology. Wiley.
Pettorelli, N., Laurance, W., O'Brien, T., Wegmann, M., Nagendra, H., Turner, W., 2014. Satellite remote sensing for applied ecologists: opportunities and challenges. https://doi.org/10.1111/1365-2664.12261
Rogers, K., Lymburner, L., Salum, R., Brooke, B., Woodroffe, C., 2017. Mapping of mangrove extent and zonation using high and low tide composites of Landsat data. Faculty of Science, Medicine and Health - Papers: part A 1–20. https://doi.org/10.1007/s10750-017-3257-5
Roy, P.S., 1989. Spectral reflectance characteristics of vegetation and their use in estimating productive potential. Proc. Indian Acad. Sci. (Plant Sci.) 99, 59–81. https://doi.org/10.1007/BF03053419

Saintilan, N., Rogers, K., Mazumder, D., Woodroffe, C., 2013. Allochthonous and autochthonous contributions to carbon accumulation and carbon store in southeastern Australian coastal wetlands. Faculty of Science, Medicine and Health - Papers: part A 84–92. https://doi.org/10.1016/j.ecss.2013.05.010

Schuerch, M., Vafeidis, A., Thomas, S., Temmerman, S., 2013. Modeling the influence of changing storm patterns on the ability of a salt marsh to keep pace with sea level. Journal of Geophysical Research 118. https://doi.org/10.1029/2012JF002471

Sifleet, S., Pendleton, L., Murray, B.C., 2011. State of the Science on Coastal Blue Carbon (No. NI R 11-06). Nicholas Institute for Environmental Policy Solutions.

Silvestri, S., Defina, A., Marani, M., 2005. Tidal regime, salinity and salt marsh plant zonation. Estuarine, Coastal and Shelf Science 62, 119–130. https://doi.org/10.1016/j.ecss.2004.08.010

Silvestri, S., Marani, M., 2004. Salt-Marsh Vegetation and Morphology: Basic Physiology, Modelling and Remote Sensing Observations, in: The Ecogeomorphology of Tidal Marshes. American Geophysical Union (AGU), pp. 5–25. https://doi.org/10.1029/CE059p0005

Snow, A., Vince, S., 1984. Plant zonation in an Alaskan salt marsh. II: An experimental study of the role of edaphic conditions. https://doi.org/10.2307/2260075

Spencer, T., Schuerch, M., Nicholls, R., Hinkel, J., Lincke, D., Vafeidis, A., Reef, R., McFadden, L., Brown, S., 2016. Global coastal wetland change under sea-level rise and related stresses: The DIVA Wetland Change Model. Global and Planetary Change 139. https://doi.org/10.1016/j.gloplacha.2015.12.018

Swoish, M., Da Cunha Leme Filho, J.F., Reiter, M.S., Campbell, J.B., Thomason, W.E., 2022. Comparing satellites and vegetation indices for cover crop biomass estimation. Computers and Electronics in Agriculture 196, 106900. https://doi.org/10.1016/j.compag.2022.106900

Temmerman, S., Govers, G., Wartel, S., Meire, P., 2004. Modelling estuarine variations in tidal marsh sedimentation: Response to changing sea level and suspended sediment concentrations. Marine Geology 212, 1–19. https://doi.org/10.1016/j.margeo.2004.10.021

Tempfli, K., Huurneman, G.C., Bakker, W.H., Janssen, L.L.F., Feringa, W.F., Gieske, A.S.M., Grabmaier, K.A., Hecker, C.A., Horn, J.A., Kerle, N., Meer, F.D. van der, Parodi, G.N., Pohl, C., Reeves, C.V., Ruitenbeek, F.J.A. van, Schetselaar, E.M., Weir, M.J.C., Westinga, E., Woldai, T., 2009. Principles of remote sensing : an introductory textbook, 4th ed, 2. International Institute for Geo-Information Science and Earth Observation.

Testa, S., Soudani, K., Boschetti, L., Borgogno Mondino, E., 2018. MODIS-derived EVI, NDVI and WDRVI time series to estimate phenological metrics in French deciduous forests. International Journal of Applied Earth Observation and Geoinformation 64, 132–144. https://doi.org/10.1016/j.jag.2017.08.006

Turner, R.K., Bateman, I.J., Georgiou, S., Jones, A., Langford, I.H., Matias, N.G.N., Subramanian, L., 2004. An ecological economics approach to the management of a multi-purpose coastal wetland. Reg Environ Change 4, 86–99. https://doi.org/10.1007/s10113-004-0075-x

Ungar, I.A., 1991. Ecophysiology of vascular halophytes. CRC Press, Boca Raton.

Ursino, N., Silvestri, S., Marani, M., 2004. Subsurface flow and vegetation patterns in tidal environments. Water Resources Research 40. https://doi.org/10.1029/2003WR002702

US EPA, O., 2015. Classification and Types of Wetlands [WWW Document]. URL https://www.epa.gov/wetlands/classification-and-types-wetlands (accessed 6.16.22).

Van de Broek, M., Temmerman, S., Merckx, R., Govers, G., 2016. Controls on soil organic carbon stocks in tidal marshes along an estuarine salinity gradient. Biogeosciences 13, 6611–6624. https://doi.org/10.5194/bg-13-6611-2016

Wang, H., Wal, D., Li, X., van Belzen, J., Herman, P., Hu, Z., Ge, Z.-M., Zhang, L., Bouma, T., 2017. Zooming in and out: scale-dependence of extrinsic and intrinsic factors affecting salt marsh erosion: Factors on salt marsh edge erosion. Journal of Geophysical Research: Earth Surface. https://doi.org/10.1002/2016JF004193

Willemsen, P.W.J.M., Smits, B.P., Borsje, B.W., Herman, P.M.J., Dijkstra, J.T., Bouma, T.J., Hulscher, S.J.M.H., 2022. Modeling Decadal Salt Marsh Development: Variability of the Salt Marsh Edge Under Influence of Waves and Sediment Availability. Water Resources Research 58, e2020WR028962. https://doi.org/10.1029/2020WR028962

Xue, J., Su, B., 2017. Significant Remote Sensing Vegetation Indices: A Review of Developments and Applications. Journal of Sensors 2017, 1–17. https://doi.org/10.1155/2017/1353691

Yang, J., Paytan, A., Yang, Y., Wei, S., Liu, B., Cui, H., Chen, Y., Zhao, Y., 2020. Organic carbon and reduced inorganic sulfur accumulation in subtropical saltmarsh sediments along a dynamic coast, Yancheng, China. Journal of Marine Systems 211, 103415. https://doi.org/10.1016/j.jmarsys.2020.103415

ANNEX

Table 1 Values of AGB, BGB, Bulk density and LOI for each plot and their respective bio are shown, together with their sum and average. They are organized according to their species associations.

Species Ass+ GPS lociations	AGBs g/m2	BGB g/m2 Mean (0-30 cm of depth)	Bulk Density (g/cm3)	LOI%
Sarcocornia >= 80%				
P8B1	1280.75	5008.96	0.46	15.28
P8B2	739.50	5451.61	0.52	12.17
P8B3	1520.75	8717.49	0.48	13.23
Average P8	**1180.33**	**6392.69**	**0.49**	**13.56**
GPS21	1003.00			
GPS24	1343.75			
GPS25	2378.00			
Average Species association	**1377.63**			
Limonietum (Limonium >= 80 %)				
P1B1	299.50	6777.47	0.59	13.95
P1B2	357.75	5430.02	0.46	15.71
P1B3	298.00	6272.37	0.50	16.35
	318.42			
P2B1	545.75	7219.51	0.51	15.07
P2B2	395.00	6601.99	0.64	10.62
P2B3	464.50	4175.56	0.48	14.71
	468.42			
P5B1	589.25	8976.91	0.45	18.68
P5B2	529.00	4950.24	0.44	14.58
P5B3	528.00	6472.93	0.36	15.35
	548.75	**6319.67**	**0.49**	**15.00**
GPS20	278.75			
GPS22	494.75			
Average Species association	**434.57**			
Spartina maritima >= 20 % and <= 70%				

P7B1	332.00	5506.90	0.38	16.63
P7B2	388.50	4635.75	0.39	17.42
P7B3	189.25	4365.05	0.38	7.98
	303.25	**4835.90**	**0.38**	**14.01**
GPS2	388.00			
GPS8	707.00			
GPS11	396.75			
GPS12	476.75			
GPS13	521.25			
Average Species association	**424.94**			
Spartina maritima = 100%	**1044.16**			
GPS6	1029.75			
GPS15	2297.00			
Average GPS	**1663.38**			
including the 100 density				
Juncus >= 80%				
GPS16	1556.75			
GPS18	766.25			
Average GPS	**1161.50**			
Inula >= 50%				
P10B1	1496.25	4781.05	0.56	11.79
P10B2	589.00	3841.56		
P10B3	191.25	2639.33	0.72	9.41
Average P10	**758.83**	**3753.98**	**0.64**	**10.60**
GPS17	1289.00			
GPS19	853.00			
GPS23	967.75			
Average Species association	**897.71**			
Spartina anglica >= 90%				
P4B1	481.25	2649.04	0.38	0.49
P4B2	365.75	1683.36	0.39	14.75
P4B3	315.50	3047.21	0.42	15.17

P4B3	315.50	3047.21	0.42	15.17
Average P4	**387.50**			
P6B1	297.00	1715.76	0.61	10.97
P6B2	312.00	1317.68	0.49	12.52
P6B3	413.25	1837.18		
Average P6	**340.75**	**2041.71**	**0.46**	**10.78**
GPS9	384.75			
GPS14	360.00			
Average Species association	**366.19**			
Salicornia veneta > 30% w Soil				
P3B1	152.00	1861.31	0.49	11.92
P3B2	144.25	1434.55	0.49	11.93
P3B3	237.25	2011.62	0.48	15.28
Average P3	**177.83**			
P9B1	221.00		0.51	4.49

P9B2	177.75	1839.17	0.32	3.24
P9B3	70.25	615.05		
Average P9	**156.33**	**1552.34**	0.46	9.37
GPS1	526.50			
GPS4	176.75			
GPS5	236.75			
GPS7	126.75			
Average Species association	**206.93**			

Table- 2 Represents the mean values of the spectral curves used to compute the indices NDVI; SAVI; MSAVI and GEMI. The values are shown for each species association.

Dominant species	RED	NIR	BGB	AGB (g/m2)	NDVI	SAVI	MSAVI	eta	GEMI
Lim. nar.	0.052	0.304	2898.10	318.41667	0.709	0.442	0.427	0.772	0.701
Lim. nar.	0.048	0.298	3340.10	468.41667	0.721	0.443	0.428	0.762	0.697
Sal	0.071	0.179	1315.90	177.83333	0.433	0.217	0.185	0.478	0.479
Sp. ang.	0.061	0.341	1960.00	387.5	0.696	0.465	0.457	0.850	0.737
Lim. nar.	0.044	0.265	8976.90	548.75	0.716	0.410	0.387	0.688	0.654
Sp. ang.	0.076	0.294	1715.80	340.75	0.590	0.376	0.354	0.737	0.654
Sp. mar.	0.065	0.201	5506.90	303.25	0.509	0.265	0.231	0.530	0.523
Sar. fr.	0.079	0.394	5009.00	1180.3333	0.666	0.486	0.483	0.954	0.777
Sal	0.068	0.176	1839.20	156.33333	0.442	0.218	0.185	0.472	0.477
In. crit.	0.049	0.221	4781.10	758.83333	0.636	0.335	0.302	0.584	0.578